Structural Models of the KtrB, TrkH, and Trk1,2 Symporters Based on the Structure of the KcsA K^+ Channel

Stewart R. Durell and H. Robert Guy
Laboratory of Experimental and Computational Biology, Division of Basic Sciences, National Cancer Institute, National Institutes of Health, Bethesda, Maryland 20892-5677 USA

ABSTRACT Three-dimensional computer modeling is used to further investigate the hypothesis forwarded in the accompanying paper of an evolutionary relationship between four related families of K^+ sympoter proteins and the superfamily of K^+ channel proteins. Atomic-scale models are developed for the transmembrane regions of one member from each of the three more distinct symporter families, i.e., a TrkH protein from *Escherichia coli*, a KtrB protein from *Aquifex aeolicus*, and a Trk1,2 protein from *Schizosaccharomyces pombe*. The portions of the four consecutive M1-P-M2 motifs in the symporters that can be aligned with K^+ channel sequences are modeled directly from the recently determined crystal structure of the KcsA K^+ channel from *Streptomyces lividans*. The remaining portions are developed using our previously accumulated theoretical modeling criteria and principles. Concurrently, the use of these criteria and principles is further supported by the now verified predictions of our previous K^+ channel modeling efforts and the degree to which they are satisfied by the known structure of the KcsA protein. Thus the observed ability of the portions of the symporter models derived from the KcsA crystal structure to also satisfy the theoretical modeling criteria provides additional support for an evolutionary link with K^+ channel proteins. Efforts to further satisfy the criteria and principles suggest that the symporter proteins from fungi and plants (i.e., Trk1,2 and HKT1) form dimeric and/or tetrameric complexes in the membrane. Furthermore, analysis of the atomic-scale models in relation to the sequence conservation within and between the protein families suggests structural details for previously proposed mechanisms for the linked symport of K^+ with Na^+ and H^+. Suggestions are also given for experiments to test these structures and hypotheses.

INTRODUCTION

The accompanying paper presents evidence for a homologous relationship between the superfamily of bacterial K^+-channel proteins and several families of K^+ symporter proteins (Durell et al., 1999). These include 1) the TrkH subunit of the Trk system from both bacteria and archaea (Schlösser et al., 1995; Stumpe et al., 1996; Nakamura et al., 1998a); 2) the KtrB subunit of the KtrAB system from bacteria (Nakamura et al., 1998b) (previously identified as NtpJ; Takase et al., 1994; Clayton et al., 1997), and 3) an ad hoc group from eukaryotes (called Trk-euk) combining the Trk1,2 family from yeast and neurospora (Gaber et al., 1988; Ko and Gaber, 1991; Lichtenberg-Fraté et al., 1996; Haro et al., 1998, unpublished (accession no. AJ009758)), the HKT1 protein from wheat (Schachtman and Schroeder, 1994), and a homologous putative K^+ symporter from *Arabidopsis* (Washington University Genome Sequencing Center, 1998 (*A. thaliana* Genome Sequencing Project, http://genome.wustl.edu/gsc/arab/arabidopsis.html); Bevan et al., 1999 (EU *Arabidopsis* Sequence Project, unpublished; accession no. CAB39784)).

In this paper, the homology hypothesis is further examined through the development of representative models of one member from each of the three K^+ symporter families. In the past, we have used computer graphic and energy minimization methods to develop atomic-scale models of membrane proteins, with emphasis on K^+ channels. By necessity, these models have been constrained only by a series of theoretical modeling criteria and the results of indirect structural experiments. Here we use an alternative homology modeling approach, in which development of the K^+ symporter models is based primarily upon the crystal structure of the KcsA channel, using alignments of the sequences with that of the KcsA and other bacterial K^+ channels (see accompanying paper). Interestingly, it is found that the resultant homology models qualitatively satisfy our modeling criteria independently. This provides further corroboration of the homology between symporter and channel proteins and support for the use of the theoretical methods for developing unaligned regions of the symporter models. Finally, if these two superfamilies of membrane proteins are indeed homologous, then the addition of the KcsA crystal structure information should result in more accurate models than our previous efforts relying on the criteria and indirect experimental studies alone.

The Results section is divided into three parts corresponding to three categories of examined model types. In the first, schematic helical-wheel diagrams are presented that illustrate the approximate locations of the protein residues at the extracellular surface and outer half of the transmembrane region. This gives a general overview of the portions of the model symporter structures that are homologous to the K^+ channels. The second part provides greater

Received for publication 8 February 1999 and in final form 8 May 1999.
Address reprint requests to Dr. H. Robert Guy, Laboratory of Experimental and Computational Biology, National Cancer Institute, National Institutes of Health, Bldg. 12B, Rm. B116, 12 South Drive, MSC 5677, Bethesda, MD 20892-5677. Tel.: 301-496-2068; Fax: 301-402-4724; E-mail: guy@guy.nci.nih.gov.

0006-3495/99/08/789/19 $2.00

detail, with the development of atomic-scale models of all portions except for the cytoplasmic components of the symporters. Special emphasis is given to predicting possible functions for the charged residues in the transmembrane region, as well as the differences between the channel and symporter inner pore regions formed by the M2 segments. Alternative models are presented that suggest plausible conformational changes in the P_C, $M2_C$, P_D, and $M2_D$ segments. The final part presents a number of molecular schematics for the active symport process suggested by the atomic-scale models and describes how they could be tested by mutagenesis methods.

METHODS

Our criteria and principles for developing 3D models of membrane proteins are as follows (Guy and Durell, 1994, 1996):

1. Most insertions and deletions should occur in the loops connecting the transmembrane segments.
2. These loops should be poorly conserved and relatively hydrophilic if they play no important functional role.
3. Residues that are exposed to the lipid alkyl chains should be hydrophobic and poorly conserved (Guy, 1988; Komiya et al., 1988).
4. Most highly conserved residues (with the exception of residues such as some prolines that strongly affect the secondary structure) should interact with other highly conserved residues and should be structurally and/or functionally important.
5. If mutations at two positions and/or segments are highly correlated, then these two residues or segments are likely to be interacting (Göbel et al., 1994).
6. The transmembrane segments should form a solid barrier between the lipid alkyl chains and the pore.
7. The hydrophobic portions of the transmembrane segments that are exposed to lipid should begin and end in planes that are ~30 Å apart and that correspond to the transition region between the lipid headgroups and their alkyl chains.
8. Segments in contact with the lipid alkyl chains should have a regular secondary structure.
9. The net charge of the residues interacting with the internal lipid headgroups should be positive.
10. Almost all hydrogen bond donor and acceptor atoms should form hydrogen bonds with other protein groups, water, or lipid headgroups.
11. Although not essential, preference should be given to structures that allow charged residues in the transmembrane region to be near to, or form salt bridges with, oppositely charged residues.
12. Transmembrane helices that are sequentially adjacent are likely to be structurally adjacent (Bowie, 1997).
13. It should be possible to connect transmembrane helices with the shortest linking segment in the aligned sequences of the protein family.
14. In packing transmembrane α-helices, a preference should be given to arrangements in which the crossing angle between adjacent helices is near 20° (Bowie, 1997).
15. Most backbone and side-chain conformations should be energetically favorable and occur frequently in proteins of known conformation (Ponder and Richards, 1987).

Atomic-scale models of the symporters were developed in the following manner. Idealized α-helices were generated for those segments of the symporters that align in sequence with the helices of the KcsA crystal structure. The side chains of the residues were initially set into the conformation that occurs most often for them in α-helices in the protein structure database. These symporter helices were then positioned in 3D space according to the known KcsA channel structure. Side-chain conformations were then adjusted to avoid steric overlap, and in some cases, to form energetically favorable interactions such as salt bridges and hydrogen bonds. The nonhelical segments, such as P2, that could be aligned with the KcsA structure were again modeled directly according to the crystal structure conformation. The remaining segments, e.g., linkers connecting M1 to P1, P2 to M2, and the four MPM motifs, were modeled according to the above-listed theoretical "rules." Subsequences of connecting segments with high calculated probabilities of forming an α-helix were given this conformation. It is important to note that, as reflected in the list of principles, poorly conserved loop segments are not likely to be crucial for the primary functional mechanisms of the proteins. Because we do not believe that they can be modeled accurately with current methods, arbitrary conformations are given to the remaining, nonhelical loop regions simply to demonstrate the feasibility of the models. Once an initial structure was constructed, its energy was minimized using the CHARMM computer program (Brooks et al., 1983). The resultant structure was then examined and manually adjusted to better satisfy the modeling rules. This process was iterated until subsequent small changes were insignificant.

RESULTS

Helical wheel models

Fig. 1 *A* shows a helical wheel schematic of an idealized bacterial 2TM K^+ channel as viewed from outside the cell. The helical wheels are positioned in the general locations of the protein α-helices in the outer portion of the transmembrane region of the KcsA crystal structure. The letters represent the consensus sequence of the 27 putative 2TM bacterial K^+ channels, with the side chains color coded according to the degree of conservation among these sequences, as shown in Fig. 2 *B* of the accompanying paper. Note that the order of the segments in terms of degree of conservation (i.e., P2 > P1 > M2 > M1) is consistent with their functions in the structure. For example, the P2 segments should be the most highly conserved because they form the K^+-binding sites that determine the ion selectivity of the channel. Similarly, M1 should be the least well conserved segment because it is located on the periphery of the structure, where it is mostly exposed to lipid alkyl chains and contributes only slightly to the lining of the pore. It should also be noted that for each of the α-helices (i.e., of the M1, P1, and M2 segments), the more conserved face is oriented toward the pore, while the less conserved face is oriented toward the surrounding lipid. This can also be seen as the pattern of residues becoming less well conserved as a function of distance from the pore, which lies at the center of the assembled tetramer.

The large red-to-orange colored circles in the background of Fig. 1 *A* indicate positions in which the same residue is conserved among the K^+ channels and all three, two, or one of the symporter families. These residues are located throughout the core of the outer transmembrane portion of the protein illustrated in Fig. 1. In addition to the cluster of four highly conserved glycines from the four P2 segments, many residues of this category are found buried within each subunit between the M1, P1, and M2 segments.

From the statistical analysis in the preceding paper it was found that the KtrB subunit family is the most similar of the K^+ symporters in sequence profile to the bacterial 2TM K^+ channels for three of the four MPM motifs: i.e., MPM_A, MPM_C, and MPM_D. KtrB is also the symporter family in

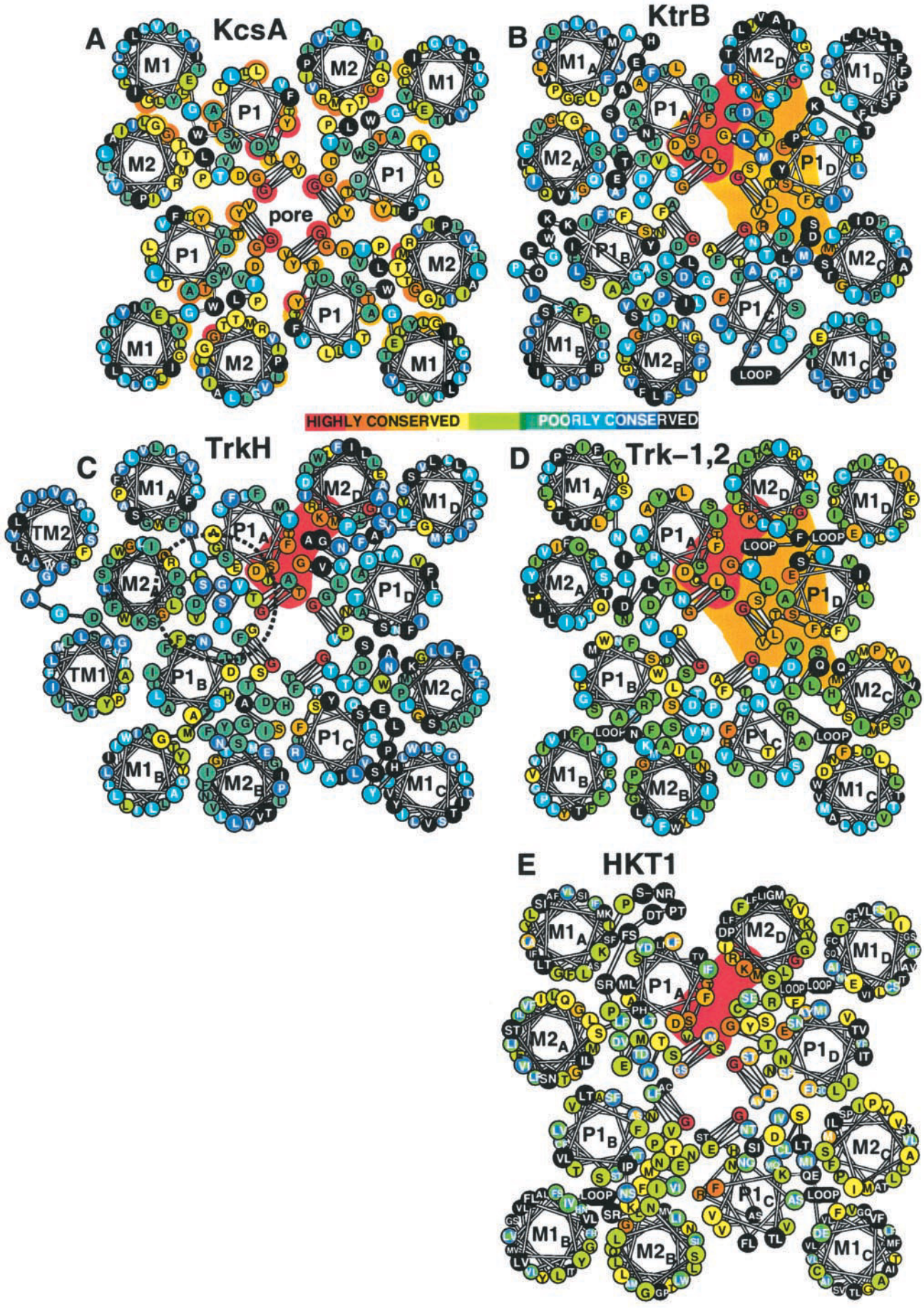
A
KcsA
M1
M2
P1
pore
B
KtrB
LOOP
HIGHLY CONSERVED
POORLY CONSERVED
C
TrkH
TM2
TM1
D
Trk–1,2
LOOP
E
HKT1

which the four MPM motifs are the most similar to each other. Accordingly, Fig. 1 *B* shows a helical wheel representation of our model of the KtrB family of symporters based on the KcsA channel structure. The residues are colored according to the degree of conservation among 18 KtrB sequences as in Fig. 2 *B* of the accompanying paper. As is clearly seen, the relationship between the structure of the symporter model and the degree of conservation of the sequences is very similar to that of the channels. When ranked according to their degree of conservation, the order of the four main segments is the same as that of the K^+ channels (i.e., P2 > P1 > M2 > M1). Again, the faces of the helices oriented toward the pore are more highly conserved than those oriented toward the lipid. Moreover, most of the highly conserved residues of the KtrB symporters—many of which are either identical or very similar to analogous highly conserved residues in the channels—interact in the model with other highly conserved residues.

The schematic in Fig. 1 *C* shows a situation similar in most respects for the TrkH family, but with a few notable exceptions. These are that the outwardly oriented faces of $M2_A$ and $P1_B$, and to a lesser extent that of $M1_A$, which are conserved relatively well compared to those of the KtrB family. Interestingly, except for one known species of KtrB (see accompanying paper), the TrkH family also deviates by the existence of two additional transmembrane helices, called TM1 and TM2, preceding the MPM_A motif. Thus our explanation for the higher degree of conservation of the outwardly oriented faces of $M2_A$ and $P1_B$ in TrkH is that they interact with the TM1 and TM2 helices rather than with the more fluid, lipid alkyl chains. This is accomplished in the model by having the more highly conserved TM1 α-helix packed next to the $M2_A$ and $P1_B$ segments, and having the less well conserved TM2 α-helix packed with greater membrane exposure next to the $M1_A$ and $M2_A$ segments. We also postulate (see below) that the $M2_A$ and $P2_B$ segments of the TrkH family may be involved in the H^+ permeation pathway, because of the hydrophilic nature of their residues (*area bound by dashed line*). Their ability to perform this function could be affected by their interaction with TM1. In addition, the number of residues that are conserved between symporter families is less for TrkH than for the other two families in the outer portion of the transmembrane region. Excluding the glycines on P2 and M2, most of the conserved residues occur in a cluster where $P1_A$ packs next to $M2_D$, as indicated by the red background in Fig. 1 *C*.

The P segments of the Trk-euk family are quite similar to those of the KtrB family, and residues that are conserved between KtrB and Trk-euk all occur in the core region. Trk-euk is the family of symporters for which the four MPM motifs are least similar to those of the bacterial 2TM K^+ channels. It is also the family in which the M1 and M2 segments of the four motifs are least similar to each other or to those of the other symporters. This suggests that only the core region involving the P segments and residues that interact with them have been conserved from the putative K^+ channel ancestor. The helical wheel representation of the Trk1,2 family (Fig. 1 *D*) indicates that the pattern of conservation differs substantially among its M1 and M2 segments. Most notably, the $M1_D$ segment is quite well conserved on all sides, which suggests that $M1_D$ is not exposed to lipids. Moreover, the external faces of the segments on each side of $M1_D$ are more highly conserved than analogous faces of helices on the opposite side of the protein. In addition, portions of $M1_D$ and $M2_D$ on the cytoplasmic side of the transmembrane region are more polar than analogous segments of the bacterial symporters, or even among the other MPM motifs of the Trk-euk symporters (in fact, the hydrophobic portion of this $M2_D$ is only eight residues long). Coincidentally, the Trk-euk proteins apparently lack additional transmembrane segments, and at present, they are not known to interact with other proteins. Our proposed explanation for these observations is that the Trk-euk symporters may function as dimer or tetramer complexes, in which the conserved sides of each monomer are buried between the protein subunits rather than being exposed to bulk lipid. Furthermore, the Trk1 and Trk2 proteins in *Saccharomyces* could interact with each other to form a heterodimer or heterotetramer. These possibilities will be described in detail below.

Although there are still only two known sequences of Trk-type K^+ symporters from plants (HKT1 from wheat and *Arabidopsis*), the helical wheel model of these proteins in Fig. 1 *E* exhibits a similar pattern of sequence conservation. The $P1_A$-$M2_D$ region (*red background*) that is conserved among all of the other symporters is also conserved in these two. The core region with residues similar to those

FIGURE 1 Helical wheel representations of the model structures of the (*A*) bacterial 2TM channels, (*B*) KtrB symporters, (*C*) TrkH symporters, (*D*) Trk1,2 symporters, and (*E*) HKT1 symporters. Each wheel represents an α-helix viewed down its axis from outside the cell. The small circles around the wheels are the single-letter codes for the consensus sequences. Each residue is color coded according to the degree of conservation within its respective family, and for the transporters, between the families as shown in Fig. 2 *B* of the accompanying paper. (*A*) The position of the helices and P2 segments are based as close as possible to the crystal structure of the KcsA K^+ channel. Note that the P2 segments, which determine the ion selectivity, are the most highly conserved. In addition, note that almost all of the helices naturally occur with their most conserved, polar faces oriented toward the pore, and subsequently, with their least well conserved, nonpolar faces toward the membrane lipid. The red-to-orange colored background circles indicate residues that are the same in all three (*red*), two (*red-orange*), or one (*yellow-orange*) of the symporter families. (*B–E*) The red background indicates regions with residues conserved among all of the symporters, and the orange background indicates residues conserved among only the KtrB and Trk-euk (i.e., Trk1,2 + HKT1) families. The dashed line in *C* indicates a region that is composed primarily of hydrophilic residues in TrkH and mostly of hydrophobic residues in the other structures. For the residue circles in *E* with two colors, the inner color and first letter are for HKT1 from wheat, and the outer circle and second letter are for the putative symporter of *Arabidopsis*.

of KtrB is slightly larger than in the Trk1,2 model, because the inwardly oriented residues of these plant $M2_A$ segments are more similar to those of the KtrB and TrkH families.

Ordering of the four MPM motifs

In developing these models according to the KcsA channel structure, it was necessary to order the four putative MPM motifs around the axis of the pore. The lengths of the cytoplasmic segments linking the four MPM motifs are sufficiently long to allow any permutation. After examining other possibilities, we settled upon models in which the MPM motifs are ordered about the pore in a counterclockwise manner when viewed from outside of the cell. The modeling rule (see Methods) that sequentially adjacent domains or motifs usually pack next to each other would allow for either clockwise (CW) or counterclockwise (CCW) arrangements, but CW models turned out to have significant disadvantages. The CW models did not satisfy the criteria for clustering highly conserved residues together as well as did the CCW models. For example, in the CCW models, especially of the TrkH family, highly conserved residues in $P1_A$ pack next to highly conserved residues on $M2_D$, and the packing of $M2_A$ next to $P1_B$ allows both of these highly conserved helices to interact with TM1. Furthermore, the CCW models of the Trk1,2 symporters provide for a more distinct pattern of residues conserved on two adjacent sides of the protein monomer (described above), which is consistent with the hypothesis that Trk-euk forms a tetramer to satisfy modeling rule 3 (Methods). In contrast, none of these favorable interactions can occur in the CW models.

Atomic-scale models

KcsA structure

Although the helical wheel schematics provide a convenient method for visualizing the general distribution of residues, they are also somewhat misleading. For example, the α-helices in the KcsA crystal structure are all tilted with respect to the axis of the pore, as illustrated in Fig. 2. Because of this, M2 moves much closer to the axis of the channel and

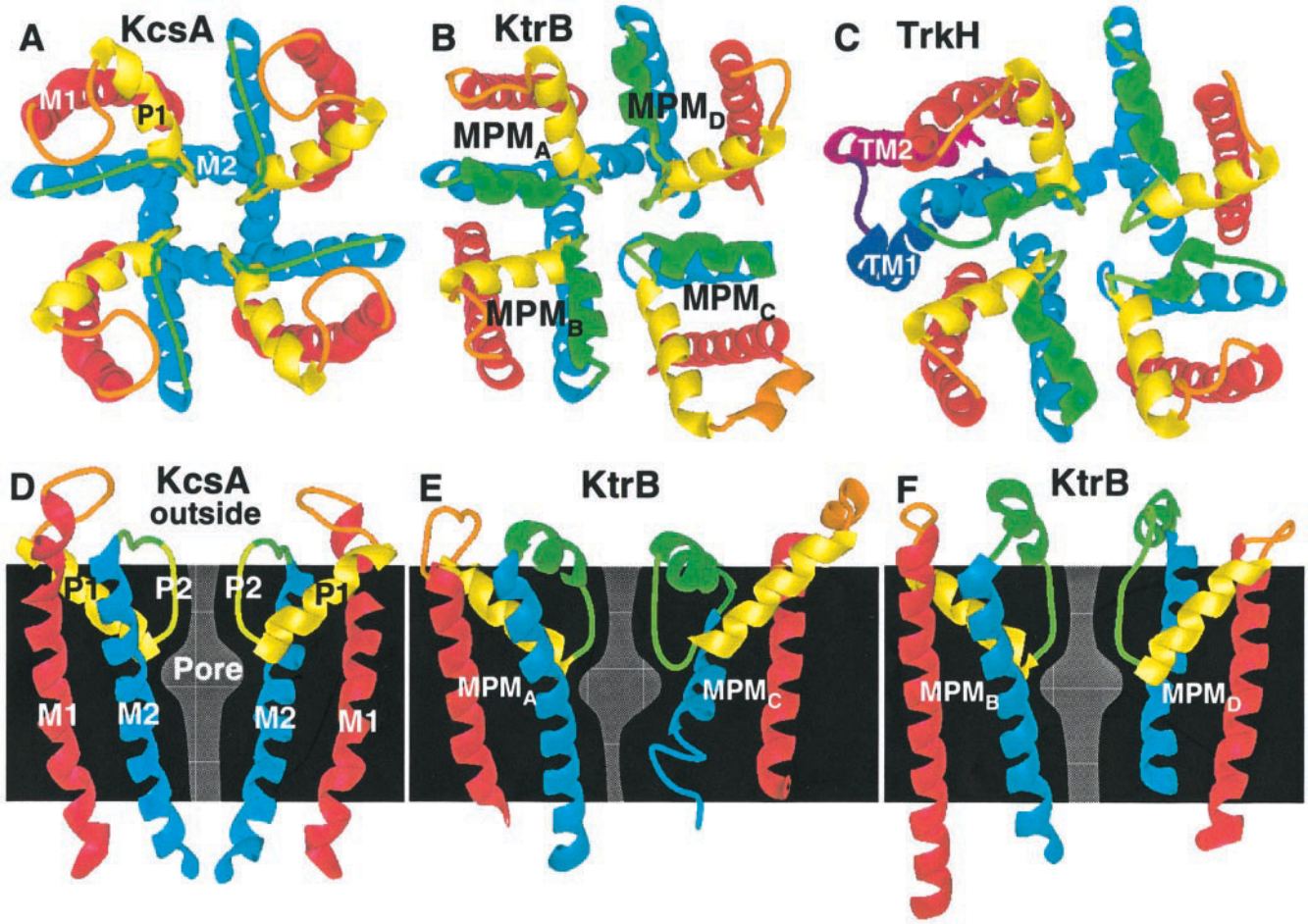

FIGURE 2 Backbone ribbon representations of the KcsA crystal structure and models of the KtrB and TrkH symporters. (*A–C*) Top view, from outside the cell, of (*A*) KcsA, (*B*) KtrB, and (*C*) TrkH. (*D*) Side view of two opposing subunits of KcsA. Side view of the (*E*) MPM_A and MPM_C motifs and (*F*) MPM_B and MPM_C motifs of KtrB. The backbones of all primary symporter segments are similar to those of the channels, except for the more cytoplasmic portions of $M2_C$ and $M2_D$ (see text for details). Alternative models for these and the symporter P_C segments are described later in the text and in Fig. 8.

is more buried in the cytoplasmic half of the transmembrane region (i.e., the region not spanned by the P segments). In addition, the recent availability of the KcsA crystal structure now allows for evaluation of the validity of our modeling criteria and principles for a member of the K^+ channel superfamily. For example, in the KcsA structure the crossing angles between the M1 and M2 helices, and between the P1 helix of one subunit and the M2 helix of the adjacent subunit, are both found to be ~15°, which is in agreement with modeling rule 14 (Methods). However, the crossing angles between the M1 and P1 helices and between adjacent M2 helices are both found to be negative but still cross each other in a manner consistent with "knobs into holes" (Crick, 1953) or "ridges into grooves" (Chothia et al., 1981) helix packing theories. Thus this rule is not absolute and only reflects the statistical preference for helix-helix crossing angles within the database of known protein structures. Similarly, although there is agreement between modeling rule 12 and the fact that the sequentially adjacent helices in the MPM motif are also structurally adjacent in the crystal structure, this may only reflect the limited ways of arranging the three helices of the channel subunit in 3D space. Thus, in developing the symporter models, which contain at least 12 helices within the single transmembrane sequence, we considered it acceptable to violate this principle for the helices between adjacent MPM domains.

The relationship between residue-residue interactions and the degree of conservation is illustrated in Fig. 3, where the residues of the KcsA structure have been colored as in Fig. 1 *A* (i.e., according to their degree of conservation among bacterial 2TM K^+ channels). The cross-sectional views demonstrate clearly that modeling rules 1–4 and 6–9 (Methods), which concern the locations and functional importance of conserved residues, are well satisfied. Although not apparent in the figure, rule 10 for hydrogen bond donors and acceptors is also well satisfied.

Modeling rule 11, concerning the formation of salt bridges, is more difficult to evaluate, because two of the charged side chains (Arg^{64} and Glu^{71} of P1) were not included in the crystal structure. Instead, we have modeled these residues to avoid artificial cavities in the structure. Arg^{64}, on the initial part of P1, can be placed so that its guanidinium group forms a salt bridge with Asp^{80} at the end of P2. It can also be modeled near Glu^{71} but is too far away

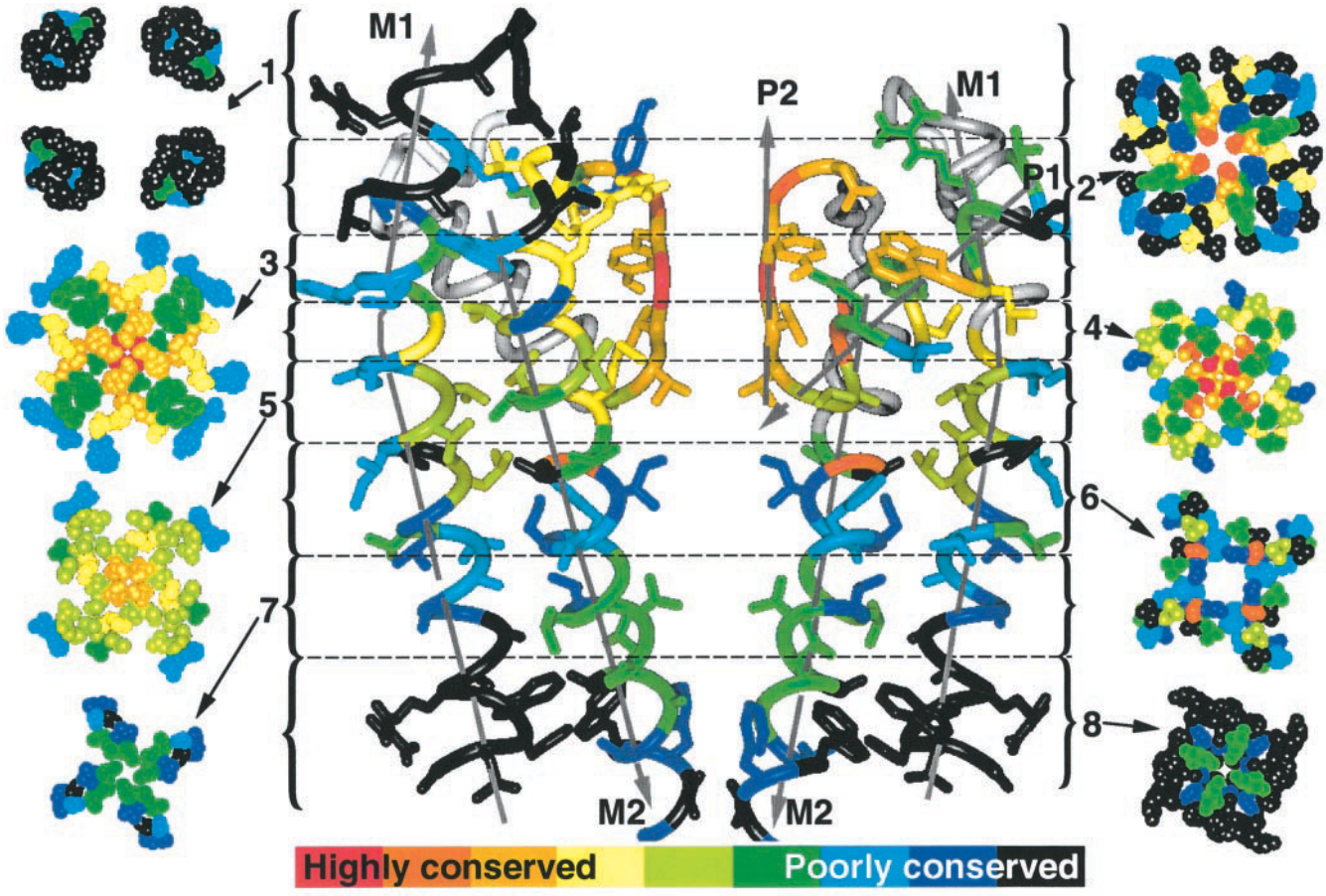

FIGURE 3 Crystal structure of the KcsA channel colored according to the degree of conservation, as in Fig. 1 *A*. The central portion is a tube-and-stick representation of two opposing subunits viewed from the side. To avoid confusion, backbone portions that are located behind other segments are portrayed in white and without side chains. The space-filling representations on both sides of the figure are cross-sectional slices through the four subunits of the channel, looking from outside the cell down the axis of the pore. The locations of the slices are indicated by the dashed lines in the side view. See text for a description of how this structure is consistent with our modeling criteria.

to directly bind. The side chains of the other two charged residues, Glu^{51} at the end of M1 and Arg^{89} on the fourth position of M2, bind to opposite sides of the backbone linking P2 to M2, but do not form a salt bridge. The charged guanidinium group of Arg^{89} is almost close enough to the carboxyl group of Asp^{80} to form a salt bridge. In summary, most charged side-chain groups are near oppositely charged side-chain groups, but some do not form salt bridges.

Symporter models

Rather than using the consensus sequences to build atomic-scale models of the symporters (as given in Fig. 2 of the accompanying paper), we decided to focus on single representative proteins from each family. For the KtrB family the member from *Aquifex aeolicus* (GenBank accession no. AE000743) was selected because this species of bacteria is thermophilic (living at 98°C; Deckert et al., 1998) and thus is likely to have exceptional folding stability. For the TrkH family the member from *Escherichia coli* (SwissProt. accession no. P21166) was selected, because this specific symporter has been extensively studied experimentally. However, for the Trk-euk family the member from the yeast *Schizosaccharomyces pombe* (SwissProt. accession no. Q10065) was chosen arbitrarily.

It should be noted that the relatively large evolutionary distances between the channels and symporters (see accompanying paper) are likely to result in numerous errors in the symporter models at the atomic scale. Nevertheless, these models are considered sufficiently accurate for analyzing the feasibility of various structures, for predicting residues and/or segments that are functionally important, and for designing appropriate experimental tests. They are also applicable for the development of structural hypotheses and experiments to test the mechanisms of K^+ symport.

Ribbon diagrams of the KtrB and TrkH models are compared to that of the KcsA crystal structure in Fig. 2. The backbone structures of the symporter models are very similar to that of KcsA at the outer portion of the transmembrane region, because we have assumed that the backbone structures are essentially identical for the primary segments, where the sequences can be aligned with little ambiguity. These include all of the M1 segments; the P segments, except for a deletion of one residue at the inner portion of P_C in the KtrB and Trk-euk proteins (see below); and the M2 segments, except for the C-terminal halves of $M2_C$ and $M2_D$ (see below). Unfortunately, the degree of sequence divergence is such that it was impossible to model these latter two exceptions after the KcsA structure in a plausible manner, or even in the same conformation for all of the symporters. Rather, a pragmatic approach was taken for these inner, pore-forming portions of the $M2_C$ and $M2_D$ segments, which is described below.

In the extracellular region, the linker sequence between the M1 and P1 segments is also extremely variable even within the protein families and thus cannot be modeled accurately from the KcsA structure. Although these loops are unlikely to be very important to the overall structure of the protein, they have been included in the models to demonstrate that the primary segments can be connected in a reasonable manner. The shortest M1-P1 linkers occur in MPM_C of the TrkH symporters from two archaebacteria: *Methanococcus jannaschii* and *Methanobacterium thermoautotrophicum*. Using the sequence of the first as an example, we have chosen to model this portion as indicated by the following alignment with the consensus sequence of the 2TM K^+ channels:

```
M. jannaschii:   ISIKDK----VPIID
2TM channels:    GTVGYYLIEGWSLFD
                 -----M1-|    |-P1
```

Whereas the linker sequence is longer in the KcsA protein (not shown), the M1 and P1 segments in the bacterial channel model were formed directly from the KcsA crystal structure. As seen by the underlines in the alignment that indicate helical conformation, the short linker of *M. jannaschii* can be reasonably accommodated by reducing the length of the $M1_C$ helix by one turn, making the second lysine the C-cap residue. This leaves the $P1_C$ segment unaffected, which is desirable, considering its importance to the transport process. This is also supported by the occurrence of a proline as the N-cap of the $P1_C$ helix, which is a common role of this residue observed for the helices in known protein structures. Thus all of the symporters should be able to form a connection between the M1 and P1 segments, given this overall structural fold, thus satisfying modeling rule 13 (Methods).

All linkers between the ion-selective portion of the P2 segment and M2 are longer in the symporters than in most of the channels. To accommodate the additional residues in a simple and reasonable manner, we postulate that the symporter P2-M2 linkers have an α-helical conformation instead of the more extended structure found in the KcsA channel. These putative helices are amphipathic and are oriented in the models with the hydrophobic residues buried between the P and M2 segments, and with the hydrophilic residues facing outward, where they are exposed to water.

Similarly, the long cytoplasmic linkers are the most speculative and ill-defined portions of the symporter models. Yet many of these sequences are also consistent with their forming amphipathic α-helices. Although we have constructed models that include these segments consistent with the modeling rules (Methods), these cytoplasmic linkers are not included in Fig. 3 because of conformational uncertainty. (The segments are included in Fig. 4, however, simply to compare the conservation of residues in the different cross-sectional views.)

Fig. 4 shows space-filling cross-sectional slices of the channel and three symporter family models. The residues are colored as in Fig. 1, i.e., according to the degree of conservation within and between the families. The surface residues of both the water-accessible loops and the lipid-exposed transmembrane helices are poorly conserved, except for some segments of Trk-euk that will be discussed

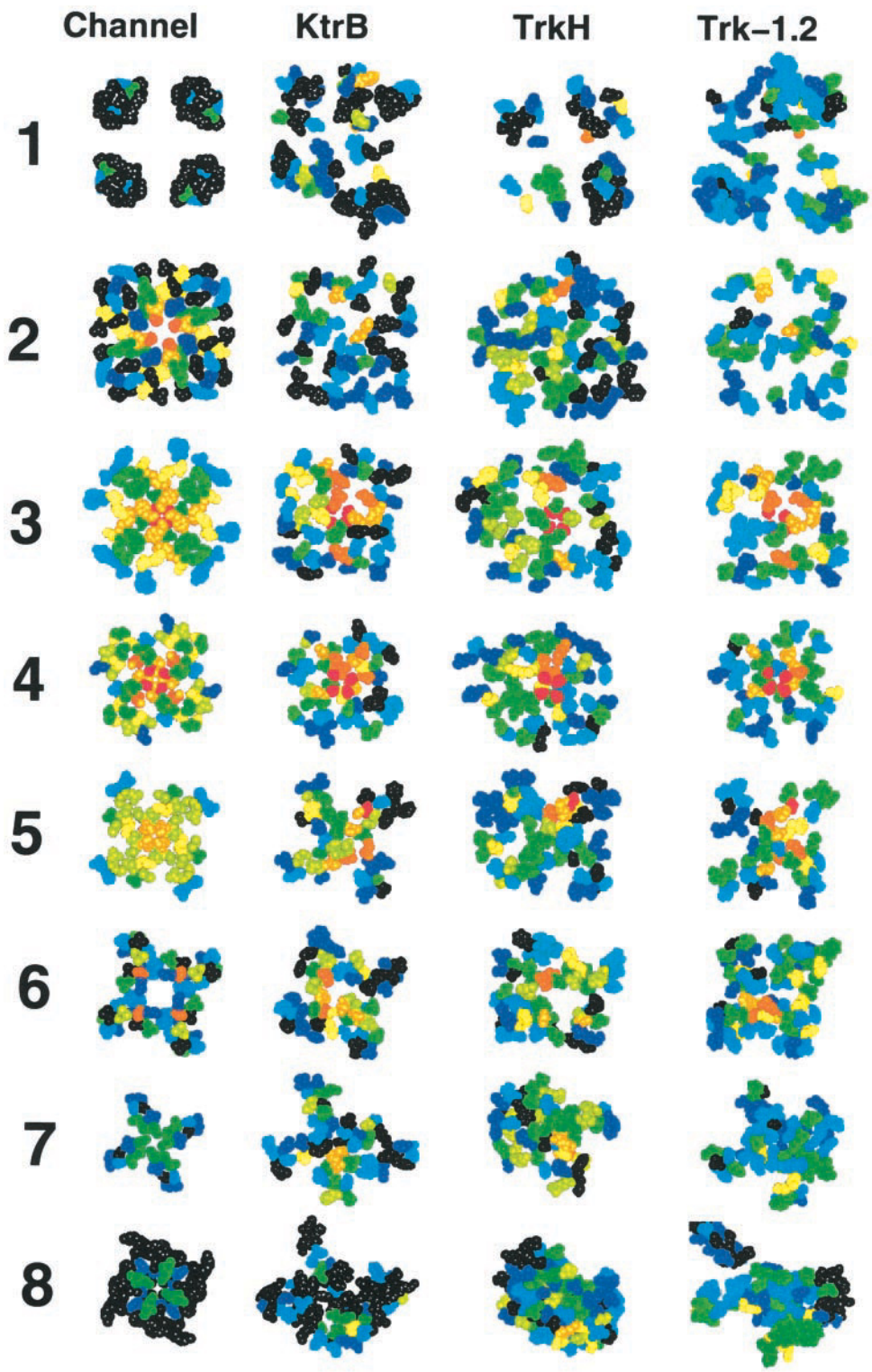

FIGURE 4 Comparison of cross-sectional slices through the channel structure and the three symporter family models. Residues are colored according to degree of conservation, as in Fig. 1. The slices through the transporters are in locations analogous to those of the channel (which are the same as in Fig. 3).

later. The cross sections in the transmembrane region illustrate that the residues that line the pore are highly conserved, that the hydrophobic core of the protein is densely packed, and that a solid barrier exists between the pore and the lipids in both models. Positively charged residues occur at the cytoplasmic lipid headgroup region of cross sections 7 and 8.

The outer entrance to the pore is not conserved in the symporters as well as in the K^+ channels. Such a result is to be expected for a pore formed by a single subunit, rather than by four identical subunits like the channel proteins. In the former case, one mutation alters only a single residue, whereas in the latter case it alters four residues oriented symmetrically around the axis of the pore. This is similar to

what occurs in the TWIK family of 2 × 2TM K^+ channels, which possess two MPM motifs within each subunit and are presumed to form dimeric channels. For example, in the P2 segment of the first motif the position normally occupied by tyrosine (Y), in the highly conserved GYGD segment forming the channel's selectivity filter, is instead often phenylalanine or leucine (similar to the symporter proteins). Likewise, in the second MPM motif the position normally occupied by aspartate (D) in this sequence is instead very poorly conserved (H. R. Guy, unpublished observations). The position occupied by the second P2 glycine at the outer entrance to the ion-selective region in the K^+ channels is usually replaced by a small noncharged hydrophilic residue (often serine) in many of the symporter MPM motif repeats. As discussed in the section on transport mechanisms, this change may result in the loss of the outermost K^+ binding site that exists in the channel proteins.

Multimeric models of Trk-euk

The high degree of conservation of residues on the outer surface of the Trk1,2-symporter models and the relative polarity of the more inward portions of $M1_D$ and $M2_D$ in this family led to the development of models in which two or four of the monomers form a dimer or tetramer complex. Fig. 5 *A* shows a helical wheel representation of the tetramer model, in which one of the salient features is that residues buried between the monomer subunits are much more highly conserved than those on the exterior of the protein that face the lipids. More details of this arrangement emerge from the backbone ribbon diagram (Fig. 5 *B*) and the atomic-scale model, displayed as cross sections in Fig. 5 *C*. The four monomers pack tightly throughout the outer half of the transmembrane region, requiring only very modest alterations of connecting loop conformations and of the $M1_D$ helix position. Most Trk1,2 proteins have two cysteines near the end of the $M2_D$ segment located on opposite sides of the helix (see Fig. 1 *D*). In the tetrameric models these residues could form disulfide bridges that link the monomer to each of its adjacent neighbors. Support for this model comes from the fact that many of the $M1_D$ side chains that are exposed in the monomer are aromatic, and in the tetramer complex they form what are known to be energetically favorable aromatic-aromatic packing interactions. This in-

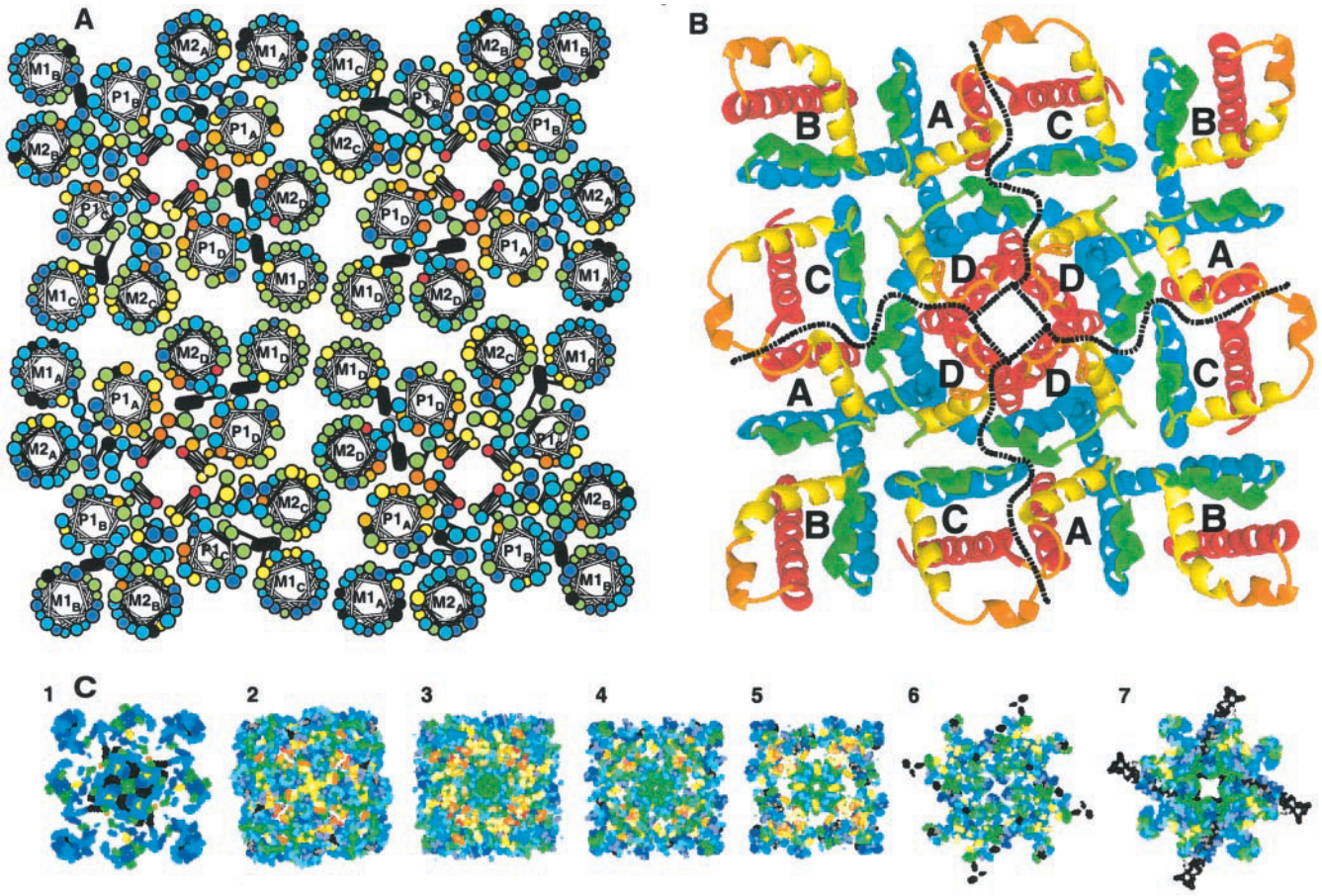

FIGURE 5 A tetrameric model for the Trk1,2 family of symporters. (*A*) A helical wheel representation of the tetramer. The color code is the same as in Fig. 1 *D*. Note that residues located at the monomer interfaces are more highly conserved than those on the surface that are exposed to lipids. (*B*) A backbone ribbon representation of the tetramer. (*C*) Space-filling cross-sectional slices through the tetramer. Note that the monomers pack tightly throughout the outer portions of the transmembrane region (*cross sections 1–5*), especially for the $M1_D$ segment. The crossing angles of the four $M1_D$ helices are typical of a coiled-coil structure.

cludes a highly conserved tryptophan residue, which forms the final contact between the four $M1_D$ helices where they begin to separate at the center of the tetramer.

In summary, the tetramer hypothesis solves several modeling problems involving the unique MPM_D motif of the Trk1,2 symporters. Specifically: 1) that $M1_D$ is conserved better than the other M1 segments because all of its surfaces are involved in protein-protein interactions, 2) that the $M1_D$ and $M2_D$ segments are more polar than in the other symporter families because they are not exposed to the lipid alkyl chains, and 3) that the hydrophobic portions of these segments are shorter than in the other symporters (e.g., the hydrophobic portion of $M2_D$ comprises only eight residues in Trk1,2) because they do not need to span the lipid bilayer.

We have also developed dimer models in which the axis of twofold symmetry is located between MPM_C and MPM_D. The dimer models appear superior for the plant symporters, whereas the tetramer models appear slightly better for the Trk1,2 family.

Interactions of charged residues

There are no positions in which a charged residue is identical among the full set of symporter sequences! However, the transmembrane regions do have several arginines and lysines (positively charged) and several glutamates and aspartates (negatively charged) that are conserved within individual symporter families (see Fig. 6). If positive residues embedded within the bilayer were unpaired, they could form an electrostatic barrier to the passage of cations through the symporters. Thus, to minimize this potential problem we have selected folding patterns that allow almost all of these residues to form salt bridges with, or at least lie near to, negatively charged glutamate or aspartate residues.

The best-conserved charged residue among all three families of symporters is an arginine near the middle of $M2_D$. (The only known exceptions are in Trk1's from *Saccharomyces cerevisiae* and *Saccharomyces bayanus* that have a similar positively charged lysine residue substitution, and in KtrB's from *Mycoplasma pneumoniae* and *Mycoplasma genitalium* that have a glutamine substitution.) Unfortunately, no one way of modeling this segment for the three symporter families could be found that is completely satisfactory in having the conserved arginine residue form a salt bridge; therefore, two alternative structures are described here. In the first, the position of the $M2_D$ segment is kept the same as in the KcsA crystal structure according to the alignment in Fig. 2 of the accompanying paper. In this conformation, the conserved arginine extends into the wide, water-filled cavity just beyond the P segments on the intracellular side of the pore (see Fig. 7 *A*). In the Trk1,2 symporters the arginine is able to form a salt bridge with the negatively charged residue that is always at one of two adjacent positions at the end of $P1_B$, and in the TrkH symporters it is able, with some distortion of the helix, to form a salt bridge with a conserved glutamate two residues beyond on $M2_D$. However, an analogous salt bridge cannot occur for the KtrB symporter family. Alternatively, the second model repositions the $M2_D$ segment from the location in the KcsA crystal structure. Specifically, the N-terminal portion of $M2_D$ (up to the conserved arginine) is shifted four positions toward the extracellular surface, and the C-terminal portion (beyond the arginine) is shifted three positions in the same direction. This places the arginine out far enough to form a salt bridge with a glutamate on the $P1_D$ segment of all KtrB and Trk-euk symporters and to approach a glutamate residue in the $P1_A$ segment of all TrkH symporters. Furthermore, with some further distortion beyond the arginine, a glycine residue and a phenylalanine residue in the $M2_D$ segment of many KtrB symporters can be positioned to coincide with the same two residues conserved in the KcsA M2 segment.

This example introduces the serious ambiguity in modeling the position of the $M2_D$ segments for most of the symporters. In addition to this, several of the yeast Trk1,2 symporters have a second arginine residue two positions

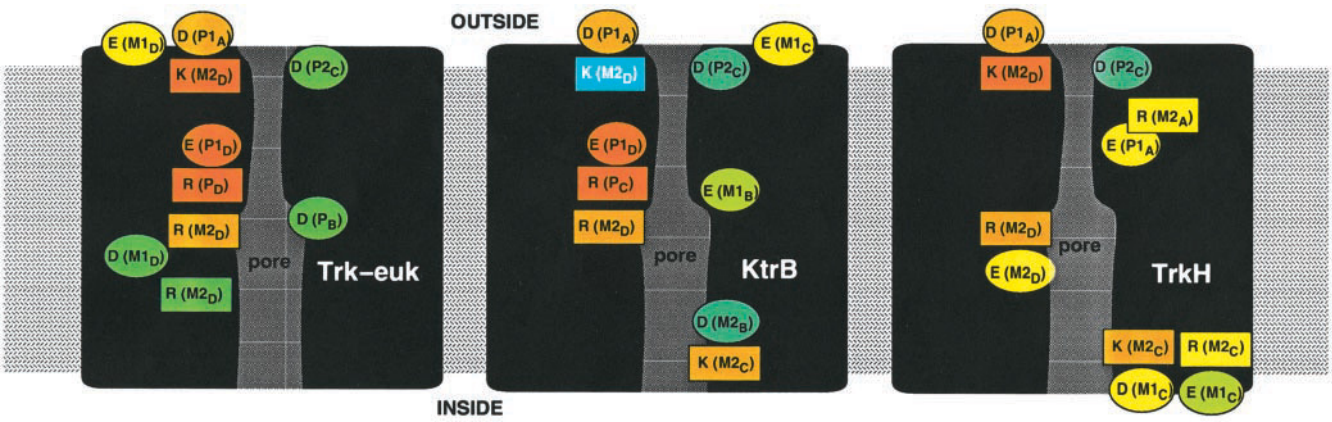

FIGURE 6 A schematic illustration of the general transmembrane locations of charged residues that are highly conserved within each family of symporters. Negatively charged residues are shown as ellipses, and positively charged residues are shown as rectangles. The residue type is indicated by the single-letter code, and the segment on which it is located is indicated in parentheses. The residues are colored as in Fig. 1.

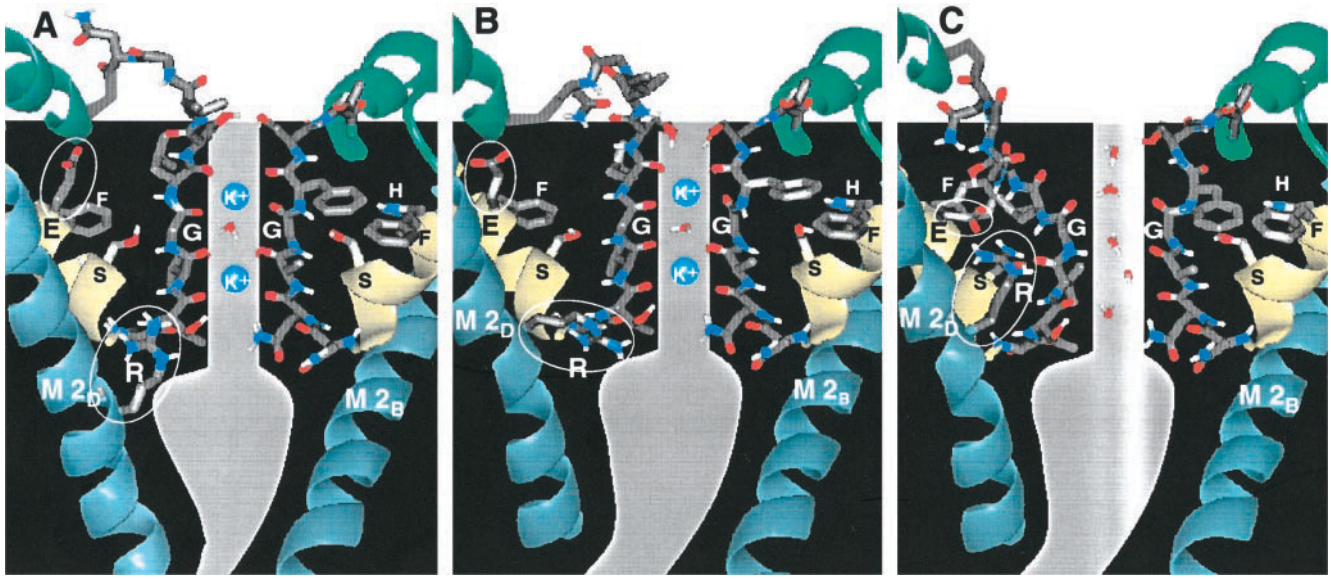

FIGURE 7 Side view of KtrB models showing $M2_D$ in different conformations. (*A*) In this model, the $M2_D$ helix is in the location suggested by its sequence alignment with the KcsA structure shown in Fig. 2 of the accompanying paper. The $M2_D$ arginine (*circled letter R*) extends into the cavity and interacts with the innermost part of the P segments. (*B*) In this model, $M2_D$ is shifted outward (toward the extracellular side) by about one turn of the helix. Its arginine side chain is oriented inwardly, where it still interacts with the innermost part of the P segments. (*C*) The backbone conformation of this model is the same as in *B*; however, the $M2_D$ arginine extends outward and forms a salt bridge with the now inwardly oriented glutamate residue of the $P1_D$ segment (*circled and labeled E*). Other side chains shown on the pore-oriented faces of the P1 segments include the phenylalanine and serine of $P1_D$, and the phenylalanine, histidine, and serine of $P1_B$. The P2 segments are shown as stick representations. Note that in *A* and *B* all of the backbone carbonyl oxygens of the P2 segments extend into the pore to form K^+-binding sites. In *C*, however, one of the P2 amide groups is oriented in the opposite direction, where its carbonyl oxygen binds to the guanidinium group of the $M2_D$ arginine.

before the highly conserved one, which in the models extends away from the pore. In the first type of model described above, where the position of the $M2_D$ segment is taken from the KcsA structure, this extra arginine can form a salt bridge with an $M1_D$-aspartate that occurs only in Trk1,2 symporters. Making this more complicated, some of the Trk1,2 symporters have yet another arginine located two residues past the highly conserved one. Interestingly, this more C-terminal arginine can form a salt bridge with the same $M1_D$-aspartate residue when the $M2_D$ segment is in the more outward position of the second type of model described above. Although the existence of multiple conformations can confound the modeling, it may also be indicative of the protein's functional mechanisms. In this case, experimental electron paramagnetic resonance studies indicate that the gating of bacterial K^+ channels involves a shift in the position of the M2 segments (Perozo et al., 1998, 1999). Thus the two possible models outlined here may actually represent a conformational change in the $M2_D$ segment involved in moving the cations through the symporters. Further implications of this notion are discussed below.

The only portion of the P segments that could not be modeled straightforwardly after the KcsA structure is the end of $P1_C$ that has a one-residue deletion in the KtrB and Trk-euk symporter sequences. Consequently, this region has been modeled in two ways. In the first, the side chain of the conserved arginine at the innermost end of the P_C segment extends outward to form a salt bridge with a glutamate residue of the $P1_D$ segment (see Fig. 8 *C*). In the plant symporters, an arginine in this position can also interact with a glutamate located immediately after the conserved glycine of $P2_C$. In the second model, the arginine side chain is in a more inward location, where it binds to the C-terminus of $P1_B$ (Fig. 8 *A*). In the Trk1,2 symporters, the arginine residue can form a salt bridge with an aspartate group occurring at one of two consecutive positions at the end of $P1_B$. The plant symporters, however, do not have negatively charged residues at this location. In the KtrB symporters, the conserved arginine in $P2_C$ lies near a glutamate on $M1_B$ or, in a few members of the family, on $M2_A$. Although the backbone structure of the second model is more like that of the KcsA channel, we tentatively favor the first because the arginine is in a more electronegative environment (especially for the plant symporters). In addition, the substitutions at the sites of the P_C arginine and the $P1_D$ glutamate are highly correlated (i.e., both of these residues occur in all KtrB and Trk-euk symporters, but neither ever occurs in the TrkH symporters), thus satisfying modeling rule 5 (Methods). The possibility of a functional conformational change between these two model structures during transport is discussed below.

Another example of correlated mutations occurs for residues buried between the P_A, $M2_A$, and P_B segments. In the K^+ channels and in our models of KtrB and Trk-euk symporters, residues in this region tend to be hydrophobic.

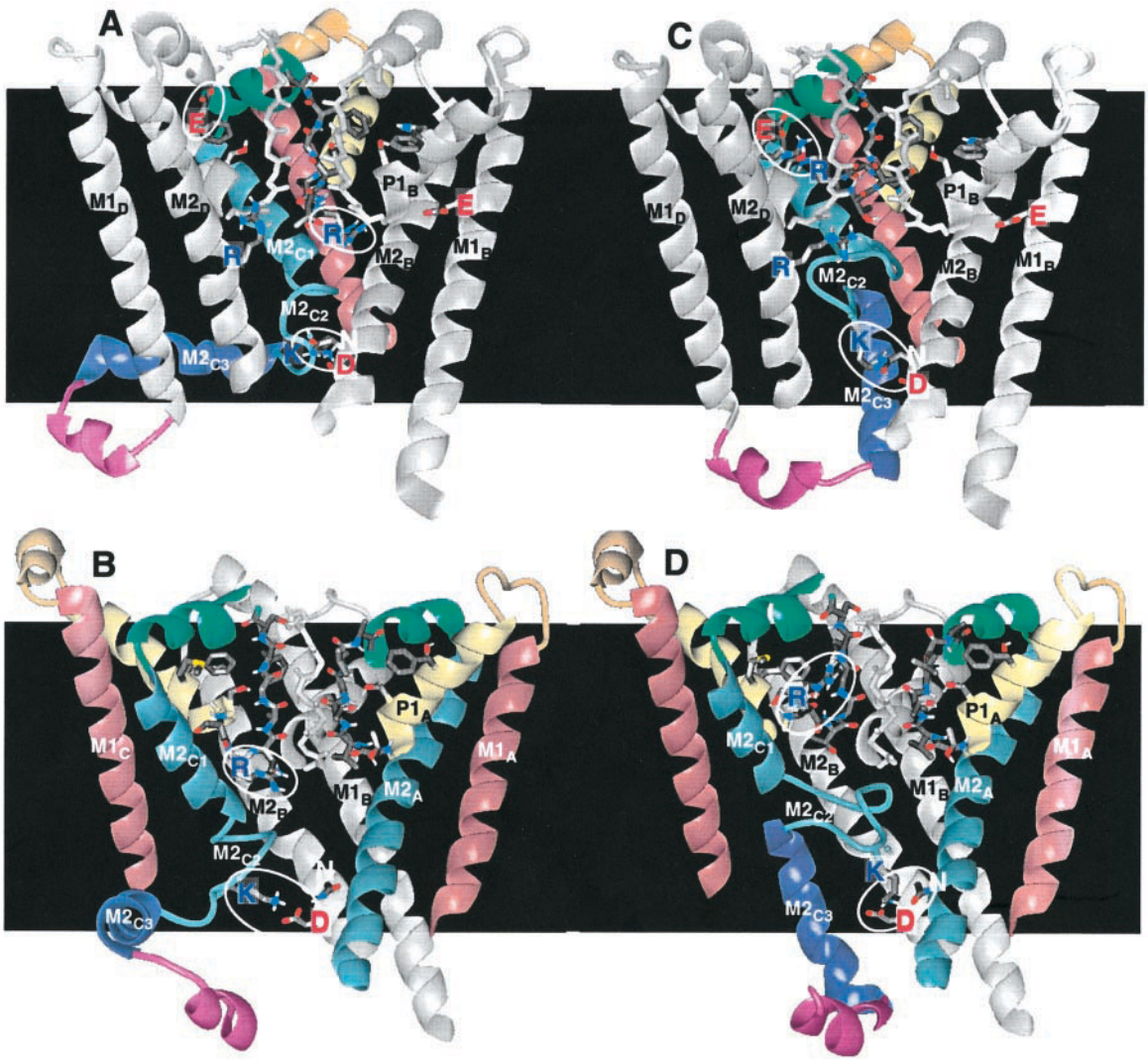

FIGURE 8 Side view of KtrB models, showing different conformations for P_C and $M2_C$ segments. In *A* and *C*, the MPM_C domain is multicolored and in the center, on the back side of the model, and MPM_A and MPM_D are all in white and on the sides. In *B* and *D*, MPM_C is on the left, MPM_A is on the right, and MPM_B is in the back and is colored white. In *A* and *B*, the P_C segment is modeled with its arginine's guanidinium group binding to the C-terminus of $P1_B$. In addition, $M2_{C2}$ spans the inner portion of the transmembrane region in a coil conformation, and $M2_{C3}$ lies on the inner surface of the membrane. In *C* and *D*, P_C is modeled with its arginine in an outward position, where it forms a salt bridge with a glutamate on $P1_D$. $M2_{C2}$ is modeled as a loop that fills the cavity located just interior to the P segments, and $M2_{C3}$ extends across the inner portion of the transmembrane region. In both models, a lysine, K, on $M2_{C2}$ forms a salt bridge with an aspartate, D, on $M2_B$. The charged residues are circled in white.

However, in the models of the TrkH symporters they are hydrophilic (see region bounded by the *dashed circle* in Fig. 1 *C*), and a $P1_A$ glutamate forms a salt bridge with an $M2_A$ arginine. These two residues are absolutely conserved among all of the bacterial TrkH symporters, but charged residues never occur at the analogous two locations in the other families. Two noncharged hydrophilic residues are also conserved in this region of the TrkH models. They are the residue located four positions past the conserved arginine on the pore-oriented face of $M2_A$, which is usually glutamine, and a residue on $P1_B$, which is usually asparagine in TrkH but is usually an aromatic residue in the channels and other symporters. The possibility that these hydrophilic residues are implicated in the proton transport mechanism of TrkH is discussed below.

Toward the extracellular surface, most of the symporter proteins have an aspartate near the beginning of $P1_A$ and a lysine near the beginning of $M2_D$. In our models, these residues are made to form a salt bridge when the $M2_D$ segment is in either of the two conformations described above, which is one of the reasons for favoring the CCW arrangement of the four MPM motifs (also described above). There is likewise a highly conserved glutamate residue on the extracellular surface just before the end of $M1_C$ in the KtrB proteins and before the end of $M1_D$ in the Trk-euk proteins. It is unlikely that these residues are crucial to a molecular process that is unique to the symporter proteins, because the bacterial K^+ channels also have highly conserved charged residues at corresponding positions on the outer surface.

Another aspartic acid residue is found in most of the symporters just past the end of the $P2_C$ segment, which again should be on the outer surface of the protein, near the potassium pore. Assuming that an insertion of two residues occurred just before this position, the symporter aspartate can be aligned with a highly conserved aspartate residue of the K^+ channels (see Fig. 2 of the accompanying paper). In the KcsA crystal structure, the carboxyl group of this residue extends inward to form a hydrogen bond with a backbone amide group that constitutes part of the outward-facing K^+ binding site. Because the same hydrogen bonding interaction can occur in the symporters models, it is possible that this $P2_C$ aspartate carboxyl group is also indirectly involved in forming a cation-binding site in these proteins as well.

The TrkH and KtrB symporters have a relatively complicated $M2_C$ segment, which we have modeled in three pieces designated as $M2_{C1}$, $M2_{C2}$, and $M2_{C3}$ (sequentially N- to C-terminal). $M2_{C1}$ is composed of 12 residues typical of the N-terminal portion of the other three M2 segments in both symporter families. $M2_{C2}$ has the following consensus sequences:

GASPGSTAGGIKTTT in KtrB,

and

GGCAGSTGGGIKIIR in TrkH,

which are composed of highly conserved residues in both families. Such sequences, rich in glycine, serine, threonine, and proline, are usually found to have random-coil and/or β-turn conformations (Chou and Fasman, 1974). With the exception of the isoleucines near the ends, these $M2_{C2}$ subsegments are not very hydrophobic. In contrast, $M2_{C3}$ has five or six poorly conserved hydrophobic residues followed by a string rich in positively charged residues. This latter pattern is again typical of the C-terminal portions of the M2 segments in most of the other MPM motifs, in both the symporter and bacterial K^+ channel families.

Because only $M2_{C1}$ was appropriate for modeling after the KcsA structure, with the same α-helical conformation of the N-termini of the other M2 segments, two alternative models were investigated for the $M2_{C2}$ and $M2_{C3}$ subsegments. In the first (Fig. 8, *C* and *D*), $M2_{C2}$ was modeled as a loop containing several β-turns, in which the first and last residues of the loop are very near each other. Then $M2_{C3}$ was modeled as an α-helix oriented approximately parallel to the axis of the pore. The N-terminus of $M2_{C3}$ is positioned very close to the C-terminus of $M2_{C1}$, so that the two segments essentially form a single hydrophobic α-helix that is distorted in the middle by the loop of $M2_{C2}$ β-turns. The positively charged residues near the end of $M2_{C3}$ in this model are well positioned to interact with lipid headgroups, and the $M2_{C2}$ loop protruding from the α-helix fills the cavity (seen in the KcsA structure) just interior to the P segments. Unfortunately, this portion of $M2_C$ cannot yet be modeled precisely, and these representations should be considered as only hypothetical. Note also that $M2_{C2}$ contains a highly conserved lysine four residues from its end, which in the KtrB symporters is postulated to form a salt bridge with a highly conserved aspartate near the end of $M2_B$. The analogous lysine in the TrkH symporters is instead postulated to interact with the C-termini of adjacent M2 segments. This allows the arginine at the end of $M2_{C2}$ that is conserved only in the TrkH family to bind to an $M2_D$ glutamate, which is also conserved only within the TrkH family. However, a potential functional problem in this model is that the pore is nearly occluded by the $M2_{C2}$ loop.

This problem is avoided in the second category of models (Fig. 8, *A* and *B*), in which $M2_{C2}$ is made to span the inner portion of the transmembrane region and $M2_{C3}$ is part of the cytoplasmic domain of the protein. In this case, the conserved $M2_{C2}$ lysine in KtrB symporters still binds to the $M2_B$ aspartate, and the analogous lysine in TrkH symporters binds to an aspartate located just before $M1_C$, leaving the arginine at the end of $M2_{C2}$ to bind to a glutamate just past the beginning of $M1_C$. Note again that these negatively charged residues are well conserved only among symporters of the same family. As shown in Fig. 8, *A* and *B*, the putative $M2_{C3}$ α-helix has been placed on the inner surface of the membrane, so that its poorly conserved hydrophobic residues still interact with lipid alkyl chains.

In contrast, the Trk-euk symporters differ greatly from the bacterial symporters in the sequence of $M2_C$, which does not contain a portion analogous to $M2_{C2}$ that is very unlikely to form an α-helix. Therefore, the Trk-euk $M2_C$ segment was modeled in a different manner, with a distortion in the center of the helix that allows its many charged residues to form salt bridges.

The highly conserved nature of this putative coiled $M2_{C2}$ segment in the bacterial symporters suggests that it has a functional importance: possibly acting as an ion shuttle, as discussed below. However, the fact that it is not conserved between the bacterial and eukaryote symporters also suggests that $M2_{C2}$ is not essential for K^+ transport. Interestingly, as described above, there is currently no evidence that Trk-euk symporters have an accessory, dinucleotide-binding subunit, which is constitutive of all known functioning KtrB and TrkH bacterial symporter proteins. This correlation suggests an interaction between the $M2_{C2}$ coil and dinucleotide-binding subunits of the latter two families. Such an interaction might modulate transitions between the two models of the $M2_{C2}$ and $M2_{C3}$ segments just described, thus effecting opening and occlusion of the central ion pore. For the TrkH proteins, which are modulated by osmotic pressure (Rhoads and Epstein, 1978), another possibility is that the $M2_C$ segment could be involved in the inactivation that occurs when the membrane is stretched.

Transport mechanisms

A major motivation for creating the symporter models is to develop experimentally testable molecular hypotheses for

their functional mechanisms. Owing to the sequence and predicted structural similarities of the MPM motifs, especially in the P2 segment, our working assumption is that the means for determining the K^+ selectivity in the symporters is similar to that in the channels. Thus passage of K^+ through the outer portion of the symporters is predicted to be via a narrow, central pore formed by the four P2 segments arranged with approximate fourfold radial symmetry around the axis. The following features of all four P segments of the symporters differ from those of the channels: 1) residues on the pore-oriented face of the P1 helix are smaller and more hydrophilic than those of the channels; 2) with the exception of $P2_D$, the residue preceding the conserved glycine tends to be smaller and more hydrophilic; 3) the Y-G-D portion of the P2 segment of the channels that forms the outer entrance of the pore tends to be replaced in the symporters by the sequence (L or F)-(S, T, or N)-X, where X indicates that the residue is not well conserved; and 4) the segment linking P2 to M2 is longer in the symporters.

To understand how these differences could affect the symport process, it is first necessary to understand how the P segments of the K^+ channel determine the selectivity for K^+. Analysis of the KcsA crystal structure reveals a series of binding sites formed by four consecutive residues of the K^+ channel "signature sequence," i.e., TVGY of the P2 segment. Specifically, these are 1) an inner site formed by the hydroxyl group of the threonine side chains and the carbonyl oxygens of the threonine, 2) an adjacent site formed by the threonine and valine carbonyl oxygens, 3) a water site formed by the valine and glycine carbonyl oxygens, and 4) an outer site formed by the glycine and tyrosine carbonyl oxygens. The chemistry of these sites is similar to that of the K^+-translocating antibiotic valinomycin (Ivanov et al., 1969; Pinkerton et al., 1969). In the channel, the carbonyl oxygens are oriented directly toward the pore, with a fourfold radial symmetry reflecting the arrangement of the four subunits around the axis of the pore. Each K^+ can be bound in a cubic cage of eight oxygen atoms, two from each of the four P2 segments. It is interesting that a water molecule is also observed to be bound in the ion-selective region of the crystal. This likely reflects a prohibitory electrostatic repulsion that would occur among four cations simultaneously bound to the closely adjacent sites. It is also indicative of the measured cotransport of water molecules with K^+ through the channels. The two innermost ion-binding sites are too near each other to be simultaneously occupied by an ion; thus they likely represent a single ion-binding region in which the ion can bind to either of the two sites.

In developing models of this region of the symporters, it was straightforward to model the amide groups of the first two ion-selective residues of P2, which corresponds to the inner binding region, directly from the KcsA crystal structure. However, the same was not true for modeling the outer binding site, for which it was difficult to find a conformation in which a K^+ could be simultaneously coordinated by eight backbone carbonyl oxygens. The primary reason for this is that the symporter sequences usually have a serine residue instead of a glycine at the end of the P2 segment (i.e., following the tyrosine of the channel binding site sequence). The importance of this second glycine to K^+ channel function is emphasized by the fact that it is conserved in almost all known sequences, except in that of two putative bacterial K^+ channels from *Chlorobium tepidum* and *Thermotoga maritima* (which again have serine at this position). Although this glycine is not seen to bind an ion in the crystal structure, it facilitates formation of the outer site by assuming a backbone conformation that is energetically unfavorable for the other, side-chain-containing amino acid residues. The functional importance of this has been experimentally demonstrated in the *Shaker* K^+ channel, where even conservative substitutions of this second glycine abolished the selectivity of K^+ over Na^+ (Heginbotham et al., 1994). An additional difference in the symporter sequences is the absence of an aspartic acid that is found in most K^+ channels at the next position (although some of the symporter motifs do have this residue two positions further toward the C-terminal). Again, it is seen in the KcsA structure that the carboxyl group of this aspartate binds to the amide group of the P2 tyrosine. This probably stabilizes the conformation of the outermost K^+-binding site and makes the region more electronegative and thus more conducive to K^+ binding. In contrast, the segment linking P2 to M2 in the symporters is modeled as an α-helix that is positioned with the positively charged N-terminus of the helix dipole pointed toward the pore (described above), which makes the outer entrance less conducive to cation binding. Taken together, these differences strongly suggest that the P segments in symporters lack the outermost K^+-binding sites that characterize the channel structures.

The ability to form K^+-binding sites is also likely to be affected by residues on the P1 helix that are oriented toward the pore and interact with the P2 segments. As is well illustrated in the KcsA structure (Doyle et al., 1998), the channels have two consecutive P1 aromatics that interact with the P2 tyrosine of the binding site sequence to form a 12-membered aromatic ring, or cuff, around the pore. This surrounding structure likely stabilizes the pore conformation and prevents ions from "leaking" through the channel protein in this outer region. While most MPM motifs of the symporters have a phenylalanine at the position analogous to the first P1 aromatic in the channels, the residue at the next position is usually hydrophilic, and in $P1_A$ of TrkH and $P1_D$ of KtrB and Trk-euk it is always a glutamate. Mutations of the $P1_A$ glutamate of HKT1 and of the phenylalanine that precedes it have been reported to alter the Na^+ transport without affecting the K^+ transport (Diatloff et al., 1998). On the next turn of the P1 helix, the residue facing the pore in most bacterial channels is a valine, leucine, or isoleucine, and in KcsA and inwardly rectifying channels of eukaryotes, it is a glutamate. In the symporters, however, residues at this position are smaller, with serine being the most common. Mutations of residues at this position in $P1_B$ (A240; Rubio et al., 1995) and $P1_C$ (N365; Rubio et al.,

1999) of HKT1 also have been reported to alter Na^+ transport. In the KcsA structure, residues at the P1 position just described interact with the residue that precedes the first glycine of the P2 segment. In the symporters, residues in this position in P2 (except for $P2_D$) also tend to be smaller and less hydrophobic (S, T,A, G,C) than analogous residues of the channels (V, I,L). In prior channel modeling efforts, in which the P region was modeled in a manner almost identical to that of the KcsA structure for the TVGY region (see Moczydlowski, 1998, for comparisons), it was noted that the binding site conformation of the P2 segments (i.e., with the backbone carbonyl oxygens pointing toward the axis) is stabilized by the presence of multiple K^+'s in the pore (Guy and Durell, 1995). When the cations are removed, the backbone can adopt different conformations, such as an extended β-strand, without substantially altering its own location or that of the side chains in the protein. The concept of small, rapid conformational changes of the P2 backbone that can be influenced by ions and/or side chains of the P1 and/or M2 segments may be relevant to some of the mechanistic models for transport presented below. Thus at least some of the P sequence variations between the symporter and channel proteins outlined here may reflect the need for different types and/or degrees of conformational changes and ion permeabilities.

Six plausible schematic models for the symport are presented in Fig. 9. In the first three, both cotransported ions move through a single central pathway. In the last three, only K^+ moves through the central pathway and the cotransported ion (Na/H^+ will be used to indicate Na^+ or H^+) moves through a peripheral pathway through the outer portion of the transmembrane region. In most of these models, the P region is postulated to change conformations. The $P2_D$ segment is the one most likely to undergo the structural

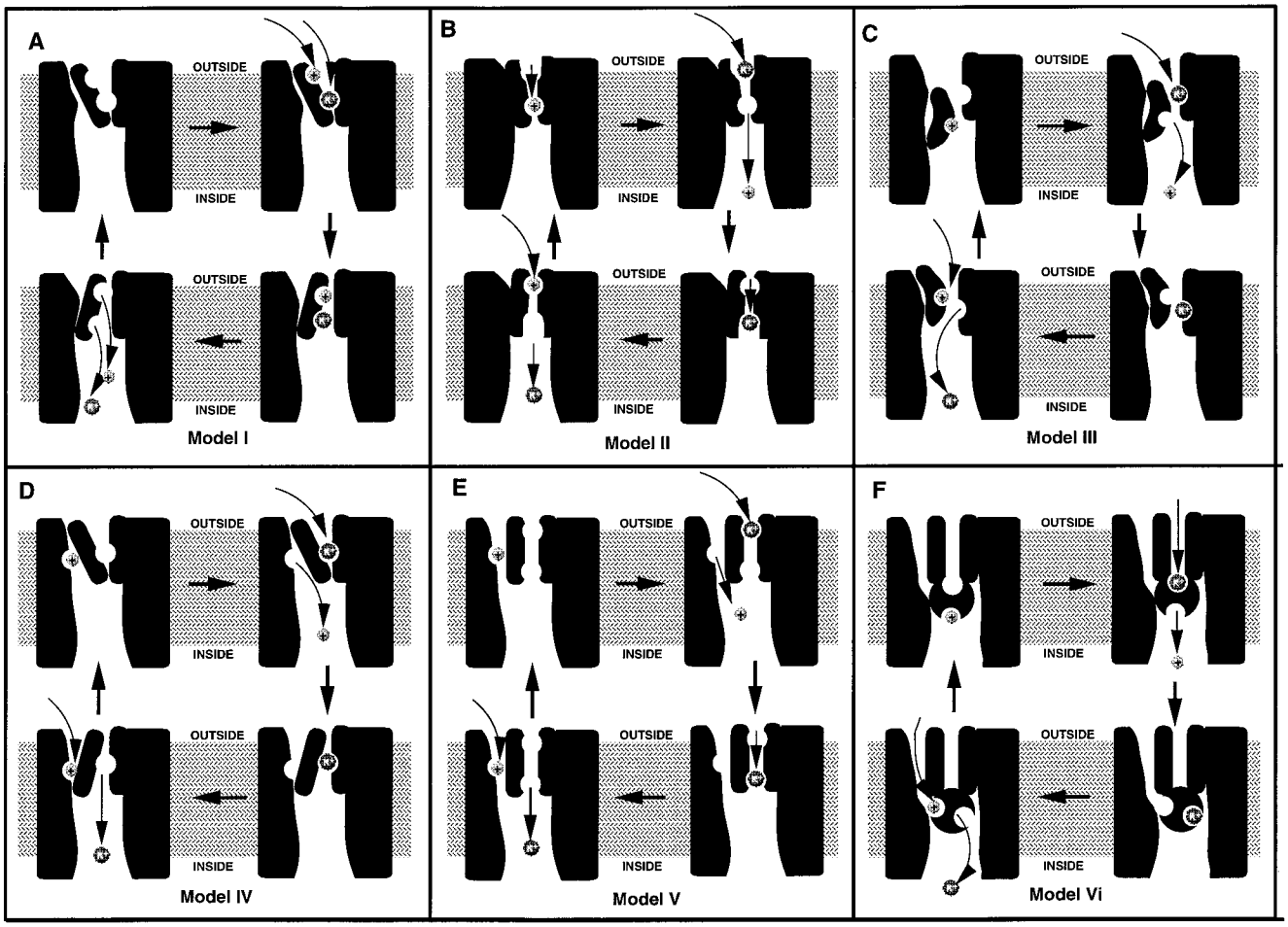

FIGURE 9 Schematic representations of plausible symport mechanisms. In all of these models, the narrow segment near the outer surface represent P2 segments with a pore in the center. The first three models have a single central pore, and the last three models have a central pore for K^+ ions and a peripheral pore for Na/H^+ ions. The barrier between the central K^+ permeation pathway and the peripheral pathway represents a P2 segment. The small spheres with a plus sign represent either H^+ or Na^+, the large spheres represent K^+, and the circular cavities represent ion-binding sites. In the first model, K^+ and Na/H^+ are simultaneously transported from an outwardly accessible location to an inwardly accessible location by movement of at least one P2 segment (and possibly other segments). In the other models, the upper conformation allows K^+ to enter and bind in the pore from the outside while allowing Na/H^+ to diffuse from the pore into the cell, and the lower conformation allows Na/H^+ to enter the pore and bind from the outside while allowing K^+ to diffuse from the pore into the cell. See text for additional details about the specific models.

transition, because it satisfies the modeling principles of being the most highly conserved among the four motifs and is located in the most highly conserved region of the combined symporter families (indicated by the *red background* in Fig. 1). Furthermore, the $P2_D$ segment is bordered on both sides by highly conserved glycine residues, which do not occur in the other three MPM motifs. In KtrB and Trk-euk the sequences following this second glycine (GLT and GYS) are quite similar to those following the first glycine (GLS and GFT), suggesting that the second sequence could move inwardly and substitute for the first after a conformational change. Glycine is the most flexible amino acid residue and is often found in regions of conformational change. However, a conformational change in P_C, such as that illustrated in Fig. 8, and a simultaneous conformational change in $M2_D$, such as that in Fig. 7, cannot be excluded.

Model I (Fig. 9 *A*) is a modification of the "alternating access" model, first articulated by Jardetzky (1966). In this case, both K^+ and Na/H^+ bind in the central P2 pore from outside of the cell. Then at least one of the P segments changes conformation so that the ions are no longer tightly bound but can only exit the pore on the cytoplasmic side of the membrane. After both ions dissociate, the symporter then reverts to the original conformation.

The other five models are drawn to have essentially identical kinetic schemes. When the symporter is in the upper conformation, K^+ binds from the outside and Na/H^+ dissociates to the inside. After this occurs, the protein moves to the lower conformation, in which Na/H^+ binds from the outside and K^+ dissociates to the inside. The models differ in which regions form the ion-binding sites and how the accessibilities of the sites from each side are determined. In these latter models the electrostatics due to the ions in the transmembrane region remain well balanced at all times, and the electrostatic repulsion from Na/H^+ can facilitate the transport of K^+ against its electrochemical gradient. In all six models, the kinetics are presumed to be driven in the clockwise direction by the movement of Na/H^+ down its electrochemical gradient.

In model II (Fig. 9 *B*) the P region has two ion-binding sites that change selectivities. In the upper conformation, the outer site binds K^+ and the inner site binds Na/H^+, whereas in the lower conformation the selectivites of the two sites reverse. This "alternating selectivity" model is similar to the "alternating access" model, except that the "gates" are replaced by sites that bind one ion type and present an energy barrier to the other ion type. This model is similar to the "multisubstrate single-file" model of Su et al. (1996), except that conformational changes are postulated to produce high-affinity ion-binding sites that should impede diffusion of ions in the "wrong" direction and to reduce energy barriers that would impede diffusion in the "right" direction. The postulated conformational changes could occur only in the P2 segments, which would be very small and quite rapid, as described above. Models that require only minor or no conformational change are more consistent with the rapid transport of ions, which has been approximated to be between 10,000 and 100,000 K^+ per TrkH complex per second (Stumpe et al., 1996). Model II differs from the others in that there are no distinct K^+ and Na/H^+ binding sites that could be identified by mutagenesis, because the same residues form sites for either ion, depending on the conformation of the protein.

Model III is similar to model II in that the locations of the postulated the K^+ and Na/H^+ binding sites relative to each other switch for the upper and lower conformations. However, in model III the switch is due to the movement of one site (the Na/H^+ site in the illustration) past the other during the conformational change. Model III is also similar to model I in that the accessibilities of the two sites alternate. However, it differs in that the two ions are not simultaneously transported from the outside to the inside by the conformational change.

In the last three models of Fig. 9, Na/H^+ is postulated to traverse the outer half of the transmembrane region through a pathway that is peripheral and parallel to the central K^+ pathway. The most likely peripheral pathway suggested by the models is between the four P1 helices that slant toward the center (see Fig. 2) and the P2 segments that are parallel to the central pore's axis. That this region is accessible to cations from outside the cell is indicated by cysteine mutagenesis experiments in K^+ channels, in which positively charged sulfhydryl reagents are found to bind to the pore-oriented face of the P1 helix when residues are replaced by cysteine (Lü and Miller, 1995; Gross and MacKinnon, 1996). This region may be more permeable to inorganic cations in the symporters because the symporters lack the bulky, aromatic cuff that surrounds the P2 pore of the channels, and because the pore-oriented faces of the symporter P1 helices and the P2 residue that precede the glycine tend to be hydrophilic and/or small amino acid residues, whereas analogous residues of the channel are larger and more hydrophobic. As mentioned above, mutations of these hydrophilic residues in $P1_B$, $P1_C$, and $P1_D$ alter the transport of Na^+ in HKT1 (Rubio et al., 1995, 1999; Diatloff et al., 1998). The models suggest that the motifs most likely to have these parallel Na/H^+ pores are MPM_D in KtrB and Trk-euk and MPM_A in TrkH, because within each symporter family they contain the P1 segments that are the mostly highly conserved, hydrophilic, and electronegative. However, contrary to the predictions of these models, mutagenesis results indicate that $P1_B$ and $P1_C$ may be involved in Na^+ transport in HKT1. It is of course possible that the symporters have multiple peripheral pathways.

Model IV (Fig. 9 *D*) is similar to model III (Fig. 9 *C*) in that one or more P2 segments change conformation so that the accessibilities from the outside and inside of the two ion-binding sites alternate. However, model IV differs in that the Na/H^+ pathway is peripheral to the central P2 pathway. The advantage of model IV is that the two ion-binding sites need not pass by each other or change binding affinities from one ion to the other.

Model V (Fig. 9 *E*) is an adaptation of the "multisubstrate single-file" model of Su et al. (1996) for symport. Their

mechanism does not require conformational change, but rather postulates that the inability of ions to pass each other in the pore permits the diffusion of one ion down its electrochemical gradient to facilitate the movement of the other ion against its gradient. The major variation in the model presented here is that the two cationic species move through separate pores in the ion-selective, outer portion of the protein. Therefore, it is assumed that the two pathways are close enough to still allow coupling of the ions, i.e., for the presence of an ion in one of the pores to prevent, by electrostatic and/or allosteric means, the other from passing by it. When this occurs the ions essentially move in a single-file manner. The advantage of this parallel-pathway model over the single-pathway model of Su et al. (1996) is that the presence of an unoccupied high-affinity binding site for one ionic species is less likely to present an energetic barrier for the passage of the other ionic species.

Model VI (Fig. 9 *F*) employs an alternative segment as a carrier or shuttle, which derives from the historically earliest proposed mechanisms for active transport proteins (i.e., binding ions on one side of the membrane and releasing them on the other). It now seems unlikely that a conformational change in the symporters carries an ion all the way across the membrane, because of the measured high rate of transport. Yet this is still an operative concept if the cations only need to be carried short distances to pass energetic barriers in the pores. Note that the version presented here differs from most other carrier models in that the selection of specific ion types need not rely on the shuttle segment itself, but is instead determined by the properties of the pores through which the ions must travel to reach the shuttle. For the bacterial symporters, the $M2_{C2}$ segment is the most likely candidate for the shuttle, because it is well located at the inner side of the P segments, is highly conserved in these two families, and contains flexible residues that could rapidly change conformation. The major flaw with this hypothesis, though, is that the $M2_{C2}$ segment of the bacterial symporters is not conserved in the eukaryote symporters (see description above).

In models I, III, and IV, the protein has two "gates," one at either end of the P segments, which prevent free diffusion of the ions through the membrane. These gates need not be steric, e.g., the positively charged arginine in P_C and/or $M2_D$ could block the inner exit from the P segments, and their outward movement, as suggested in Figs. 7 and 8, could facilitate the exit of the ions from the pore into the cytoplasm. Likewise, the residues at the ends of the P2 segment could form the gate that blocks the outer entrance to the pore. It should be noted that the real transport mechanisms of the symporters may involve combinations of some of the models presented here. For example, it is easy to envision how the connecting region between $P1_C$ and $P2_C$ or $M2_D$ could act both as a shuttle for Na/H^+ and as a gate for K^+. The point is that these conceptual and structural models may assist in the design of experiments to define the mechanism more precisely.

CONCLUSIONS

Our hypothesis that the KtrB, TrkH, and Trk-euk families of K^+ symporters have four MPM motif repeats that are homologous to the MPM motifs of K^+ channels is supported by the three-dimensional models presented here. With the exception of the extracellular loops, those portions of the symporters that span the outer half of the transmembrane region can be modeled from the backbone structure of the KcsA channel crystal structure in a manner that satisfies our modeling criteria. Although this region affects the ion selectivity of the transport process, the symporter P2 segment sequences differ too much from those in K^+ channels to predict with confidence either the existence of multiple K^+-binding sites or the relative selectivity for K^+.

Assuming that the basic hypothesis concerning the overall structure is correct, our models raise many questions about the functional mechanisms of the symporters. Do the cotransported ions pass through the same central pore or through parallel, closely coupled pores? Does transport require a conformational change and, if so, which segments and/or residues change conformations? What is the function of the charged residues in the transmembrane regions? Is the putative "loop" region of $M2_C$ involved in transport or transporter modulation? Although we suggest plausible hypotheses, the answers will come only from experimentation. Some results already indicate that the P segments are involved in the transport of both ions. To test the importance of the P2 glycines of the models presented here, Tholema et al. (1999) mutated the absolutely conserved glycine in $P2_C$ (G290) to alanine in the KtrB of *Vibrio alginolyticus*. This dramatically reduced the binding affinities of both Na^+ and K^+ without altering the maximum transport rate obtained with high extracellular concentrations of Na^+ and K^+. Furthermore, Rubio et al. (1995) have found that mutating the leucine that follows the conserved glycine in $P2_B$ alters Na^+ permeation in HKT1. Furthermore, mutations of residues on the pore-oriented faces of $P1_B$, $P1_C$, and $P1_D$ alter Na^+ transport in HKT1 (Rubio et al., 1995, 1999; Diatloff et al., 1998).

The number of methods used to study the structures of membrane proteins, especially when high-expression systems are available, is growing dramatically (see Durell et al., 1998, for review). Mutagenesis has been used extensively to study the structure and functional mechanisms of K^+ channels (for review see Durell and Guy, 1996; Durell et al., 1998). Most of the general conclusions drawn from these studies have now been validated by the KcsA crystal structure, and the same approaches could be used for the symporter proteins. Determination of the transmembrane topology of the symporters should be relatively straightforward, except perhaps for the hypothesis that the P segments span only the outer half of the transmembrane region. It should also be relatively easy to determine whether additional point mutations of suspected crucial residues in the P segments disrupt the transport process. Several mutagenesis approaches involve substitutions for cysteine, for which the

symporters should be well suited, owing to their intrinsic lack of highly conserved residues of this type (indeed, some KtrB protein sequences have only a single cysteine). These models should also facilitate studies intended to determine specific residue-residue interactions, because they indicate the relative positions and the residues that are in contact. For example, one particularly important group to study is that of the charged residues that are highly conserved in only one or two symporter families and that are predicted to form salt bridges in our models. These should be ideal candidates for the type of expression-recovery experiments that have been performed on K^+ channels to identify positively charged residues on the S4 segment that form salt bridges with negatively charged residues on S2 and S3 segments (Tiwari-Woodruff et al., 1997).

Because of the predicted similarities in structure between the symporters and the channels, it should be possible to pursue approaches that center on the production of chimera proteins. For example, the role of some or all of a symporter MPM motif sequence could be investigated by substituting it into the analogous region of a channel protein and examining the effects on conductance. For this approach, it is advisable to select a motif very similar to that of the K^+ channel, with few highly conserved residues unique to the symporter. Because of the statistical similarity in profiles (see Table 2 of the accompanying paper), MPM_B is the likely choice for the TrkH and Trk-euk families, and MPM_A for KtrB. The chances of forming a stable tetrameric channel would probably be best if the N- and C-termini were kept the same, replacing only an outer portion of the MPM motif with a symporter sequence. Another approach would be to determine whether a functional symporter could be formed by replacing one or more of its MPM motifs with that from a specific K^+ channel. Again, MPM_B should be the better choice for TrkH and Trk-euk, and MPM_A for KtrB. An added advantage of substituting out MPM_B in Trk-euk is that it does not make intersubunit contacts in any of our models of multimer complexes. Similarly, MPM_C and MPM_D would likely not be good choices for swapping out because of their high degree of conservation among the symporters and their possible roles in the transport of Na^+ or H^+. Likewise, MPM_A would not be a good choice for the TrkH symporters because of the conserved glutamate on $P1_A$ and the conserved arginine on $M2_A$ that is postulated to be important in the H^+ transport process in the peripheral channel models.

A third approach would be to attempt conversion of a symporter into a channel by replacing a putative "transporting motif" with the corresponding channel motif. A good choice for this type of experiment would be to replace MPM_C of a KtrB symporter with the MPM motif from *Helicobacter pylorii* (see Fig. 1 of the accompanying paper for sequence comparisons). A more refined experiment would be to attempt this functional conversion simply by substituting the arginines on P_C and/or on $M2_D$ with an uncharged residue. This approach might also require mutations at the ends of the P2 segments to prevent the putative "outer gate" from occluding the pore. The success of any of these conversions would support the hypothesis of structurally similar motifs and homology among the symporter and channel proteins.

The current experimental results indicate that inward diffusion of Na^+ provides the energy for transport of K^+ in the KtrB (bacteria) and HKT1 (wheat) symporters, whereas that of H^+ provides the energy in the TrkH (bacteria) and Trk1,2 (fungi) symporters. If this is true, it is potentially possible to test the roles of the P segments (and maybe the outer portions of M1 and M2) by interchanging some or all of these segments from members of the first group with those of the second. For example, our peripheral channel models suggest that Na^+-linked transport should be eliminated in KtrB if the P_D and possibly P_C segments are replaced with those from TrkH. Furthermore, it might be possible to instate H^+-linked transport by replacing all four KtrB P segments with those from TrkH (this should also include the outer portion of $M2_A$, which contains the conserved arginine in TrkH). Alternatively, a switch in selectivity between Na^+ and H^+ could be attempted by site-directed substitution of residues postulated to be important in the different symporter families.

As described in detail, the unique sequence of $M2_C$ in the bacterial symporters led to the development of two alternative possibilities for the conformation. If the model in which the N-terminus of $M2_{C3}$ binds to the C-terminus of $M2_{C1}$ is correct, then it should be possible to delete much of $M2_{C2}$ while still maintaining a functional protein. Beyond providing support for the model, this would also present a good opportunity to determine the function of the deleted subsegment. If $M2_{C2}$ acts as an inactivation ball regulated by NADH or by membrane turgor, then this deletion would likely leave the symporter constitutively active. If $M2_{C2}$ acts as an ion shuttle, then the deletion would likely transform the symporter into a channel.

We thank Evert Bakker, Tatsunosuke Nakamura, and Clifford Slayman for their many suggestions and assistance. Molecular graphics images were produced using the MidasPlus program from the Computer Graphics Laboratory, University of California, San Francisco (supported by the National Institutes of Health, RR-01081).

REFERENCES

Bowie, J. U. 1997. Helix packing in membrane proteins. *J. Mol. Biol* 272:780–789.

Brooks, B. R., R. E. Bruccoleri, B. D. Olafson, D. J. States, S. Swaminathan, and M. Karplus. 1983. CHARMM: a program for macromolecular energy minimization and dynamics calculations. *J. Comput. Chem* 4:187–217.

Chothia, C., M. Levitt, and D. Richardson. 1981. Helix to helix packing in proteins. *Mol. Biol.* 145:215–250.

Chou, P. Y., and G. D. Fasman. 1974. Conformational parameters for amino acids in helical, beta-sheet, and random coil regions calculated from proteins. *Biochemistry.* 13:211–22.

Clayton, R. A., O. White, K. A. Ketchum, and J. C. Venter. 1997. The first genome from the third domain of life. *Nature.* 387:459–462.

Crick, F. H. C. 1953. The packing of α-helices: simple coiled-coils. *Acta Crystallogr.* 6:689–697.

Deckert, G., P. V. Warren, T. Gaasterland, W. G. Young, A. L. Lenox, D. E. Graham, R. Overbeek, M. A. Snead, M. Keller, M. Aujay, R. Huber, R. A. Feldman, J. M. Short, G. J. Olsen, and R. V. Swanson. 1998. The complete genome of the hyperthermophilic bacterium *Aquifex aeolicus*. *Nature.* 392:353–358.

Diatloff, E., R. Kumar, and D. P. Schachtman. 1998. Site directed mutagenesis reduces the Na^+ affinity of HKT1, an Na^+ energized high affinity K^+ transporter. *FEBS Lett.* 432:31–36.

Doyle, D. A., J. M. Cabral, R. A. Pfuetzner, A. Kuo, J. M. Gulbis, S. L. Cohen, B. T. Chait, and R. MacKinnon. 1998. The structure of the potassium channel: molecular basis of K^+ conduction and selectivity. *Science.* 280:69–77.

Durell, S. R., and H. R. Guy. 1996. Structural model of the outer vestibule and selectivity filter of the *Shaker* voltage-gated K^+ channel. *Neuropharmacology.* 35:761–773.

Durell, S. R., Y. Hao, and H. R. Guy. 1998. Structural models of the transmembrane region of voltage-gated and other K^+ channels in open, closed and inactivated conformations. *J. Struct. Biol* 121:263–284.

Durell, S. R., Y. Hao, T. Nakamura, E. P. Bakker, and H. R. Guy. 1999. Evolutionary relationship between K^+ channels and symporters. *Biophys. J.* 77:771–784.

Gaber, R. F., C. A. Styles, and G. R. Fink. 1988. TRK1 encodes a plasma membrane protein required for high-affinity potassium transport in *Saccharomyces cerevisiae*. *Mol. Cell. Biol.* 8:2848–2859.

Göbel, U., C. Sander, R. Schneider, and A. Valencia. 1994. Correlated mutations and residue contacts in proteins. *Proteins.* 18:309–317.

Gross, A., and R. MacKinnon. 1996. Agitoxin footprinting the *Shaker* potassium channel pore. *Neuron.* 16:399–406.

Guy, H. R. 1988. A model relating the sodium channel's structure to its function. *In* Molecular Biology of Ion Channels: Current Topics in Membrane Transport, Vol. 33. W. S. Agnew, T. Claudio, and F. J. Sigworth, editors. Academic Press, San Diego. 289–308.

Guy, H. R., and S. R. Durell. 1994. Using homology in modeling the structure of voltage-gated ion channels. *In* Molecular Evolution of Physiological Processes. D. Fambrough, editor. The Rockefeller University Press, New York. 197–212.

Guy, H. R., and S. R. Durell. 1995. Structural model of Na^+, Ca^{2+}, and K^+ channels. *In* Ion Channels and Genetic Diseases. D. Dawson, editor. The Rockefeller University Press, New York. 1–16.

Guy, H. R., and S. R. Durell. 1996. Developing three-dimensional models of ion channels. *In* Ion Channels, Vol. 4. T. Narahashi, editor. Plenum Press, New York. 1–40.

Heginbotham, L., Z. Lu, T. Abramson, and R. MacKinnon. 1994. Mutations in the K^+ channel signature sequence. *Biophys. J.* 66:1061–1067.

Ivanov, V. T., I. A. Laine, N. D. Abdulaev, L. B. Senyavina, and E. M. Popov. 1969. The physicochemical basis of the functioning of biological membranes: the conformation of valinomycin and its K^+ complex in solution. *Biochem. Biophys. Res. Commun.* 34:803–811.

Jardetzky O. 1966. Simple allosteric model for membrane pumps. *Nature.* 211:969–970.

Ko, C. H., and R. F. Gaber. 1991. TRK1 and TRK2 encode structurally related K^+ transporters in *Saccharomyces cerevisiae*. *Mol. Cell. Biol.* 11:4266–4273.

Komiya, H., T. O. Yeates, D. C. Rees, J. P. Allen, and G. Feher. 1988. Structure of the reaction center from *Rhodobacter sphaeroides* R-26 and 2.4.1: symmetry relations and sequence comparisons between different species. *Proc. Natl. Acad. Sci. USA.* 85:9012–9016.

Lichtenberg-Fraté, H., J. D. Reid, M. Heyer, and M. Hofer. 1996. The SpTRK gene encodes a potassium-specific transport protein TKHp in *Schizosaccharomyces pombe*. *J. Membr. Biol.* 152:169–181.

Lü, Q., and C. Miller. 1995. Silver as a probe of pore-forming residues in a potassium channel. *Science.* 268:304–307.

Moczydlowski, E. 1998. Chemical basis for alkali cation selectivity in potassium-channel proteins. *Chem. Biol.* 5:R291–R301.

Nakamura, T., N. Yamamuro, S. Stumpe, T. Unemoto, and E. P. Bakker. 1998a. Cloning of the trkAH gene cluster and characterization of the Trk K^+-uptake system of *Vibrio alginolyticus*. *Microbiology.* 144: 2281–2289.

Nakamura, T., R. Yuda, T. Unemoto, and E. P. Bakker. 1998b. KtrAB, a new type of bacterial K^+-uptake system from *Vibrio alginolyticus*. *J. Bacteriol.* 180:3491–3494.

Perozo, E., D. M. Cortes, and L. G. Cuello. 1998. Three-dimensional architecture and gating mechanism of a K^+ channel studied by EPR spectroscopy. *Nature Struct. Biol.* 5:459–469.

Perozo, E., D. M. Cortes, and L. G. Cuello. 1999. Structural rearrangements underlying activation gating in the *Streptomyces* K^+ Channel. *Biophys. J.* 76:A149.

Pinkerton, M., L. K. Steinrauf, and P. Dawkins. 1969. The molecular structure and some transport properties of valinomycin. *Biochem. Biophys. Res. Commun.* 35:512–518.

Ponder, J. W., and F. M. Richards. 1987. Tertiary templates for proteins. Use of packing criteria in the enumeration of allowed sequences for different structural classes. *J. Mol. Biol.* 193:775–791.

Rhoads, D. B., and W. Epstein. 1978. Cation transport in *Escherichia coli*. IX. Regulation of transport. *J. Gen. Physiol.* 72:283–295.

Rubio, F., W. Gassmann, and J. I. Schroeder. 1995. Sodium-driven potassium uptake by the plant potassium transporter HKT1 and mutations conferring salt tolerance. *Science*. 270:1660–1663.

Rubio, F., M. Schwarz, W. Gassmann, and J. I. Schroeder. 1999. Genetic selection of mutations in the high affinity K^+ transporter HKT1 that define functions of a loop site for reduced Na^+ permeability and increased Na^+ tolerance. *J. Biol. Chem.* 274:6839–6847.

Schachtman, D. P., and J. I. Schroeder. 1994. Structure and transport mechanism of a high-affinity potassium uptake transporter from higher plants. *Nature.* 370:655–658.

Schlösser, A., M. Meldorf, S. Stumpe, E. P. Bakker, and W. Epstein. 1995. TrkH and its homolog, TrkG, determine the specificity and kinetics of cation transport by the Trk system of *Escherichia coli*. *J. Bacteriol.* 177:1908–1910.

Stumpe, A., A. Schlösser, M. Schleyer, and E. P. Bakker. 1996. K^+ circulation across the prokaryotic cell membrane: K^+-uptake systems. *In* Transport Processes In Eukaryotic and Prokaryotic Organisms. W. N. Konings, H. R. Kaback, and J. S Lolkema, editors. Elsevier, New York. 473–499.

Su, A., S. Mager, S. L. Mayo, and H. A. Lester. 1996. A multi-substrate single-file model for ion-coupled transporters. *Biophys. J.* 70:762–777.

Takase, K., S. Kakinuma, I. Yamato, K. Konishi, K. Igarashi, and Y. Kakinuma. 1994. Sequencing and characterization of the ntp gene cluster for vacuolar-type Na^+-translocating ATPase of *Enterococcus hirae*. *J. Biol. Chem.* 269:11037–11044.

Tholema, N., E. P. Bakker, A. Suzuki, and T. Nakamura. 1999. Change to alanine of one out of four selectivity filter glycines in KtrB causes a two orders of magnitude decrease in the affinities for both K^+ and Na^+ of the Na^+ dependent K^+-uptake system KtrAB from *Vibrio alginolyticus*. *FEBS Lett.* 450:217–220.

Tiwari-Woodruff, S. K., C. T. Schulteis, A. R. Mock, and D. M. Papazian. 1997. Electrostatic interactions between transmembrane segments mediate folding of *Shaker* K^+ channel subunits. *Biophys. J.* 72:1489–1500.